CHARACTERIZATION OF ASPHALTENES STRUCTURE: ASPHALTENE CHEMICAL STRUCTURAL CHANGES DUE TO CARBON DIOXIDE INJECTION

A Thesis

by

NIKOO GOLSHAHI

Submitted to the Office of Graduate and Professional Studies of
Texas A&M University
in partial fulfillment of the requirements for the degree of

MASTER OF SCIENCE

Chair of Committee,	Hisham A. Nasr-El-Din
Committee Members,	Jerome J. Schubert
	Mahmoud El-Halwagi
Head of Department,	Jeff Spath

August 2020

Major Subject: Petroleum Engineering

ABSTRACT

Asphaltenes precipitation during carbon dioxide injection to enhance recovery has been considered as one of the major challenges in the tertiary production phase. How CO_2 would change the asphaltenes structure is still unknown. The present study investigates the effects of CO_2 on the isolated asphaltenes utilizing various analytical techniques. Chemical structure of precipitated asphaltenes in the presence and absence of CO_2 were characterized and compared. These results were coupled with the results of the stability assessment to determine the effects of structural alteration on asphaltenes stability in the oil matrix.

Four different crude oils were used to implement this experiment. In the first step, asphaltenes were precipitated by n-heptane. The asphaltenes were then dissolved in toluene and CO_2 was injected (at 870 psi) to these solutions and they were mixed at 752°F. This process was repeated for three days, and one week to identify the effect of time on the possible reaction between CO_2 and asphaltenes at elevated temperature and pressure. Next, CO_2 was injected into the crude oils to determine whether it would react with other components of the oils other than asphaltenes. The same procedures were repeated with nitrogen as controlling experiments. For characterization, Fourier Transform Infrared Spectroscopy (FTIR spectroscopy) was conducted to specify the functional groups and their changes due to the addition of CO_2. Finally, stability alteration of precipitated asphaltenes after reaction with CO_2 was evaluated by UV-Vis spectroscopy.

FTIR results analyses demonstrated that in one tested sample the peak related to the amide functional group is created after injecting CO_2. This peak was intensified by increasing the reaction time. To characterize the origin and mechanism of amide formation, 1,4-diazabicyclo[2.2.2]octane (DABCO) was added to this asphaltenes sample during reaction with CO_2. Neither escalation of

carbonyl group nor generation of aldehyde functional group was detected in the presence of DABCO. Such an observation proves that the amide group was formed by the reaction of amine in the asphaltenes and CO_2. The stability of this sample in model oil was decreased after reaction with CO_2. On the contrary, the FTIR spectrums of the other three samples were not altered after reaction with CO_2. Interestingly, one of these three asphaltenes samples became unstable in the model oil after reaction with CO_2.

This study shows that the asphaltenes instability in the presence of CO_2 could be a consequence of either chemical structural alteration of asphaltenes or change of the oil matrix solubility. Hence a comprehensive characterization of an oil sample is essential before designing any CO_2 injection treatment. Accordingly, these results can be utilized to select more efficient inhibitors and stabilizers to prevent asphaltenes precipitation.

DEDICATION

In the name of GOD, the most merciful and compassionate

This thesis is dedicated to my beloved parents and my lovely husband.

"*Yesterday I was clever so I wanted to change the world.*

Today I am wise so I am changing myself. What you seek is seeking you."

— Jalal al-Din Rumi

ACKNOWLEDGMENTS

I would like to express my deepest appreciation to my committee chair, Dr. Hisham A. Nasr-El-Din, for providing me the opportunity to research under his supervision. I thank him for his continuous encouragement, guidance, and support throughout the course of this research. I would like also to thank Dr. Jerome Schubert and Dr. Mahmoud El-Halwagi for serving as the committee members.

I would like to thank my friends, colleagues in my research group, department faculty, and staff for making my experience at Texas A&M University a wonderful one.

I acknowledge the people who mean a lot to me, my parents, for their continued encouragement to pursue my dreams and giving me the liberty to choose what I desired. I cannot thank you enough for all the support and love you have given me. Finally, I owe special thanks to my love, Kambiz for his extreme support, love, and understanding. You were always here at times I thought that it is impossible to continue. This journey would not have been possible without everyone's encouragement.

CONTRIBUTORS

This study was supervised by a thesis committee of Dr. Hisham A. Nasr-El-Din and Dr. Jerome Schubert of the Harold Vance Department of Petroleum Engineering and Dr. Mahmoud El-Halwagi of the Artie McFerrin Department of Chemical Engineering.

All other work on the fourier-transform infrared spectroscopy (FTIR) and ultraviolet-visible spectroscopy studies for the thesis were completed by the student independently.

NOMENCLATURE

A	Absorbance
AFM	Atomic Force Microscopy
APCI	Atmospheric Pressure Chemical Ionization
API	American Petroleum Institute
ASTM	American Society for Testing and Materials
Be	Beryllium
Br	Bromine
C	Carbon
C_5	n-pentane
C_7	n-heptane
Ca	Calcium
Cl	Chlorine
CO_2	Carbon Dioxide
CT	Computer Tomography
Cu	Copper
d	Thickness, in
Da	Dalton, g/mol
DABCO	1,4-Diazabicyclo[2.2.2]Octane
EDXRF	Energy Dispersive X-ray Fluorescence
EOR	Enhanced Oil Recovery
ESI	Electrospray Ionization
F	Fluorine
FAR	Fused Aromatic Ring
FD/FI	Field Desorption/Field Ionization
FTICR-MS	Fourier Transform Ion Cyclotron Resonance Mass Spectrometry
FTIR	Fourier Transform Infrared Spectroscopy

γ	gamma
H	Hydrogen
HCl	Hydrochloric Acid
H_2O	Water
HOMO−LUMO Orbital	Highest Occupied Molecular Orbital−Lowest Unoccupied Molecular
HPLC	High-Performance Liquid Chromatography
I	Intensity, T
IFT	Interfacial Tension
IMS	Ion Mobility Spectrometry
IR	Infrared Spectroscopy
λ	Wavelength, cm
LDI	Laser Desorption/Ionization
m/z	mass-to-charge ratio
MALDI	Matrix-Assisted Laser Desorption/Ionization
MMP	Minimum Miscibility Pressure, psi
Mn	Manganese
MS	Mass Spectrometry
MW	Molecular Weight, Ib/Ibmol
N	Nitrogen
Na	Sodium
NIR	Near-Infrared
NMR	Nuclear Magnetic Resonance
P	Pressure, psi
PAH	Polycyclic Aromatic Hydrocarbon
PVT	Pressure, Volume, Temperature
ρ	Density, Ib/ft^3
RF	Recovery Factor

rpm	revolution per minute
S	Sulfur
SARA	Saturates, Aromatics, Resins, Asphaltenes
SO_2	Sulfur dioxide
T	Temperature, °F
T%	Transmittance Percentage
TOF−MS	Time-of-Flight Mass Spectrometry
TWIM	Traveling Wave Ion Mobility
U	Uranium
UV-Vis	Ultraviolet-Visible Spectrophotometry
V	Vanadium
Vol%	Volume Percentage, ft^3%
W	Wavenumber, cm^{-1}
WDXRF	Wavelength Dispersive X-ray Fluorescence
wt.%	Weight Percent, Ib%
XRD	X-ray Diffraction
XRF	X-ray Fluorescence

TABLE OF CONTENTS

Page

LIST OF FIGURES

Page

LIST OF TABLES

Page

CHAPTER I

INTRODUCTION AND LITERATURE REVIEW

Properties of Asphaltenes

Asphaltenes are the largest, heaviest and most complex fraction of crude oil that contains condensed aromatic rings with alkyl side chains, heteroatoms, like nitrogen, sulfur, oxygen, and traces amount of metals, such as nickel and vanadium (Moreira et al. 1999). Asphaltenes are the most polar and surface-active part of the oil that is defined based on a solubility regime. Asphaltenes are soluble in light aromatics such as benzene, toluene, and pyridine. however, they are insoluble in n-alkane solvents such as n-heptane (C_7) or n-pentane (C_5). The Saturates, Aromatics, Resins, and Asphaltenes (SARA) analysis begin with asphaltenes precipitation by heptane (Melendez et al. 2012).

When asphaltene was first identified, its molecular weight was the main parameter that was used for its characterization. It was the first parameter for asphaltenes identification. Nowadays, it is obvious that molecular weight couldn't be the most accurate factor for asphaltenes characterization and molecular weight should not be the only parameter for asphaltenes description. Because, the solubility of asphaltenes in pentane or heptane, polarity, aliphatic length chain and combinations of these factors help to define the asphaltenes (Sheu 2002). The asphaltene color changes from clear to deep brown or black when asphaltene content in oil grows from 0 to 20 percent (Hortal et al. 2007).

Several experiments have been conducted for finding the molecular weight (MW) of asphaltenes, including electrospray ionization (ESI), atmospheric pressure chemical ionization (APCI), and field desorption/field ionization (FD/FI). The detected asphaltenes MWs are in the range of 500-3000 Da. These results are very sensitive to the temperature, sample concentration, and type of solvent. On the other hand, much higher MWs have been identified by matrix-assisted laser desorption/ionization (MALDI) and Laser desorption/ionization (LDI). These changes in molecular weight arise from the aggregation tendency of asphaltenes molecules. Hence, higher MWs were obtained due to the aggregation (Cunico et al. 2004; Qian et al. 2007).

Pomerantz et al. (2009) used a two-step laser mass spectrometry to obtain the asphaltenes MW. In this experiment, to eliminate the aggregation effect on MW, a short pulse of low-energy photons was used. The energy of these photons is below the ionization energy of asphaltenes. Hence, all molecules are thermally desorbed very fast. Then, the neutral molecules are ionized by a higher energy laser pulse. With this technique, the highest MW distribution for asphaltenes is 1000-1500 Da. Then, Pinkston et al. (2009) published a comprehensive paper containing all the mass spectroscopies techniques. The asphaltenes average molecular weight was concluded to be 750 Da. In addition, most of the tested asphaltenes have a molecular weight of 500–1000 Da.

The problems due to the presence of asphaltenes in crude oils come from its destabilization by different factors in flow assurance. Changes in temperature and composition of crude oil are the main factors causing asphaltenes precipitation. For instance, a heavy crude oil with a high percentage of asphaltenes may not cause the asphaltenes precipitation trouble, whereas oil with less than 0.1 wt.% asphaltenes may lead to serious asphaltenes precipitation problems. Pressure depletion during primary recovery is another reason for the asphaltenes precipitation. Moreover,

CO_2 flooding can alter the phase behavior of the fluid, and consequently causes the precipitation of organic solids such as asphaltenes (Ibrahim and Idem 2004). So, the major problem of CO_2 injection is related to the asphaltenes precipitation. Asphaltenes precipitation could occur in the wellbore, reservoir, surface facilities, and subsurface formations. The thick deposit of asphaltenes can sharply decrease production by pore plugging, blocking the valves and submersible pumps, and alteration in rock wettability, which eventually causes a reduction in enhanced oil recovery (EOR) performance.

To optimize oil production, finding the asphaltenes composition and the situations in which asphaltenes remain in a solution can be beneficial. Hence, an acceptable method has been developed to fraction the crude oil components based on its polarity and solubility to saturates, aromatics, resins, and asphaltenes (SARA). The SARA method has a simple procedure that can be performed in many chemical laboratories and it is the main advantage of this separation method. However, SARA analysis has many disadvantages. The results may not be representative under actual reservoir conditions. Because the gaseous components that are lacked from dead oil can be dissolved in live oils. In addition, the solubility of asphaltenes changes with the type of n-alkane that is used as a precipitant. Although its simplicity makes the SARA analysis a widespread method for oil comparison, single oil may have two different SARA results. Therefore, to reduce the variations in SARA analysis results, the asphaltenes precipitant (type of n-alkane) should be constant for different oils.

Asphaltenes Characterization

The incomplete knowledge of asphaltenes chemical structure and their features are the challenging issues in dealing with asphaltenes in the oil and gas industry. These pieces of knowledge help the industry to obtain the most relevant techniques for inhibiting its precipitation. The early asphaltenes model named Yen model was proposed regarding the asphaltenes structure. However, major uncertainties found in this model, including the asphaltene molecular weight, molecular architecture, aggregation species, aggregation numbers, and concentration of formation. In recent years, due to specific data, the modified Yen model was proposed. It has been called the Yen-Mullins model that is shown in **Figure 1** (Mullins 2010).

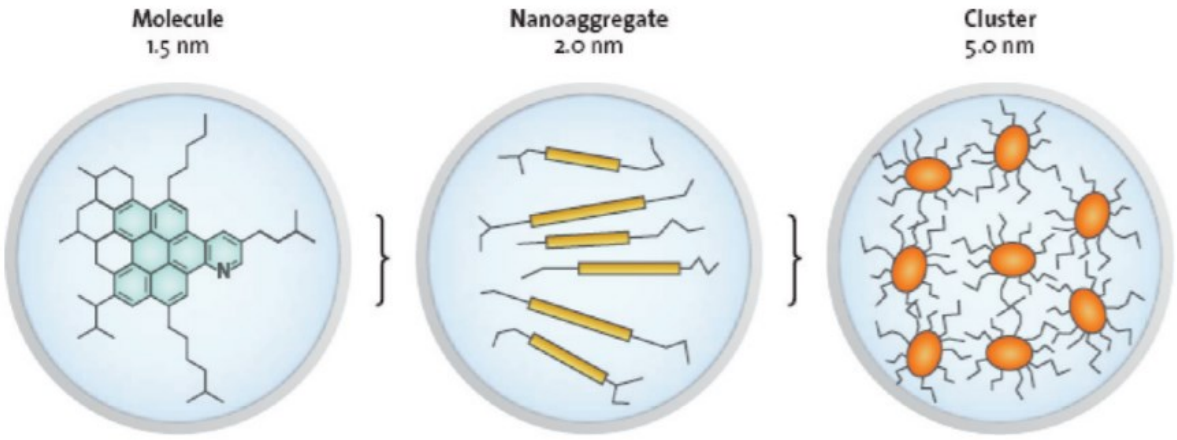

Figure 1. Yen−Mullins Model.

This model shows the dominant molecular and colloidal structures for asphaltenes. The most probable asphaltene molecular weight is ∼750 g/mol (Da), and the island molecular architecture dominates with one aromatic ring system per molecule. With sufficient concentration, asphaltene molecules form nanoaggregates with small (<10) aggregation numbers and with one disordered stack of aromatics. At higher concentrations, nanoaggregates form clusters, again with small (<10)

aggregation numbers. Based on the recent progress of the Yen-Mullins model, asphaltene aggregate structure contains fused aromatic rings (FAR), heteroatoms and alkyl groups. The FAR region in asphaltenes is similar to polycyclic aromatic hydrocarbons (PAHs) (Mullins et al. 2012).

The highest occupied molecular orbital−lowest unoccupied molecular orbital (HOMO−LUMO) gap of asphaltenes should be calculated as an index of molecular size and structure for PAHs. It has been identified that the magnitude of the (HOMO−LUMO) gap is related to the number of fused aromatic rings in the PAH region of asphaltenes. The experimental HOMO−LUMO gap range of asphaltenes is obtained from fluorescence emission data. It has been concluded that based on the HOMO-LUMO gap results, 5 FAR-10 FAR is the most common PAH size in asphaltenes structure (Ruiz-Morales 2002).

Schuler et al. (2015) found the 18 FAR and larger ring systems in asphaltenes structure by using atomic force microscopy (AFM) and scanning tunneling microscopy. The atomic-resolution imaging and molecular orbital imaging of more than 100 asphaltenes were combined. A single aromatic core with peripheral alkyl chains is the main part of the asphaltene structure. Observation of many asphaltenes with AFM showed that their structures are island structure, not the archipelago molecular structure type. The archipelago structure contains two or more PAH cores connecting with an alkane chain. The island molecular architecture of asphaltenes, where there is a single PAH core per molecule with peripheral alkanes has also been confirmed by fluorescence depolarization molecular diffusion measurements and unimolecular decomposition utilizing laser ionization mass spectrometry.

Nuclear magnetic resonance (NMR) spectroscopy is one of the main techniques for studying the asphaltenes structure. ^{1}H and ^{13}C solid and solution-state NMR are useful tools for analyzing the asphaltenes structure. The early liquid-state ^{1}H and ^{13}C NMR demonstrated that the most probable number of fused rings in asphaltenes is seven. To be more in-depth, one coal-derived asphaltene and one petroleum asphaltene has been studied by Dutta Majumdar et al. (2016) utilizing a solid-state ^{13}C NMR study. Their results showed that the asphaltene architecture ranges from small PAH cores (<5 condensed rings) to large PAH cores (>9 condensed rings). The small one is related to the coal-derived asphaltene.

Time-of-flight mass spectrometry (TOF−MS) is appropriate for the detection of asphaltene aggregates. Because it charges ions up to 20 kDa. Based on the mass analysis results, nanoaggregate and monomeric species of asphaltenes have m/z higher and lower 2000 respectively. To characterize and determine the elemental composition of lower mass species of asphaltenes, fourier transform ion cyclotron resonance mass spectrometry (FT-ICR MS) is used. Both ultrahigh-resolution FT-ICR MS and TOF−MS techniques were performed by McKenna et al. (2013) for analyzing the asphaltene aggregation with m/z≈1400. The results showed that only the most aromatic part of asphaltenes is ionized. Furthermore, most asphaltenes are non-covalently aggregated at concentrations that are detectable for most mass spectrometers.

Mass spectrometry (MS) was one of the principals and common techniques for asphaltene characterization. Furthermore, the combination of MS and chromatographic methods have been widely applied to oils and their derivatives. Ion mobility spectrometry (IMS) is a gas-phase ion separation technique in which the matters are separated based on their charges and sizes. A cell that has a weak electric field, is filled with an inert gas that is usually helium. Then, ions are

injected into the filled cells. This spectrometry worked based on the time that ions of samples needed to cross the cell. The combination of IMS with MS (IMS-MS) is developed for identifying the ion mobility of petroleum samples such as asphaltenes. Furthermore, traveling wave ion mobility (TWIM) has been introduced as a new model for IMS experiments. In TWIM, ions are accumulated and periodically released into a T-wave cell, where the transient voltage pulses (traveling waves) applied continuously to pairs of stacked ring electrodes. This technique has a high ion transmission and separation resolution (Koolen et al. 2018). These methods couldn't determine the chemical components and functional groups of asphaltenes. This study can propose the island architecture for asphaltenes.

The structure of asphaltenes can be observed by using the X-ray diffraction (XRD) spectra. X-ray peaks contain gamma-peak (γ-peak) and (002)-peak that represent alkyl chain and aromatic material respectively. In this research, the cubic solid structure should be assumed for the asphaltenes structure. For estimating the aromaticity and crystalline behavior, the asphaltene molecular dimensions should also be calculated. The positions and size of the diffraction peaks are used for characterizing the structure and crystallite size of asphaltenes. Tall narrow peaks in the XRD patterns are crystalline. On the other hand, broad peaks are related to less crystalline and smaller particle sizes (Shirokoff and Lye 2019). These types of researches need validation. Because they are based on some solid assumptions for the asphaltenes structure.

Coelho et al. (2007) utilized two infrared regions for characterizing the aromatic hydrogens of asphaltenes functional groups by FTIR tests. 700-900 cm^{-1} was the first region in which single H and paired one in the aromatic rings were characterized in the 860-900 cm^{-1} and 800-860 cm^{-1} regions respectively. 2900-3100 cm^{-1} was the second region that symmetrical and asymmetrical

stretching of aromatic hydrogens were shown. Then, the percentage of isolated H and paired H that are attached to aromatic rings of asphaltenes were calculated.

Structures of SARA fractions of crude oils were investigated by Akmaz et al. (2011). Elemental analysis, NMR, and FTIR were the analytical tools in this experiment. The distribution of carbon atoms from different fractions of oil was identified. The C=C, C=O, CH_2 and CH_3 functional groups were recognized by FTIR. Since asphaltene is a complex fraction of oil, there are still some hypotheses for its structure. The saturate fraction contained a long aliphatic chain. But the aromatic fraction consisted of aromatic groups with short aliphatic chains. On the other hand, fused aromatic rings with branched paraffin and polar compounds were observed in resins and asphaltene was the most complex fraction.

The asphaltenes from three different crude oils were analyzed by Hosseini et al. (2016) for identifying the effect of the electrostatic field on the aggregation rate and its size by using the optical microscope and a high voltage direct current power supply. Then, C, H, N, S elemental analysis and FTIR tests were conducted for finding the characterization of asphaltenes. It has resulted that the asphaltene aggregation rate is directly proportional to the number of hetero-atoms on asphaltene molecules. Aggregation size was also related to the concentration of asphaltene particles in the mixture and the voltage that applied to them. In addition, asphaltene was deposited faster under the electrostatic field. Hence, based on the literature review, FTIR was used in my present work for asphaltenes characterization due to its rapidity, low cost, sample preparation simplicity, and huge applicability. One of the main interests of the petroleum industry is determining the structure of asphaltenes. The new structural features of asphaltenes may better

explain their physical-chemical properties, affording new insights to heavy oil extraction and refining.

CO_2 Flooding

CO_2 flooding is used for increasing oil production and reducing oil viscosity in the Enhanced Oil Recovery (EOR) process in the oil field (Kokal and Sayegh 1995). CO_2 dissolution into the crude oil causes oil viscosity reduction. Hence, the irreducible oil saturation is reduced. The great amounts of residual oil can be recovered by this treatment. Oil recovery is increased by 8-16% by this process (Magruder et al. 1990). Various processes are involving in enhancement oil production by CO_2. CO_2 flooding is conducted with oil-viscosity reduction and oil-swelling effect, which causes changes in CO_2-crude oil properties such as reducing the interfacial tension and increasing the oil mobility (Srivastava et al. 1999). Another environmental benefit of CO_2 storage in the reservoir is decreasing greenhouse gas emissions (Godec et al. 2013). However, CO_2 transportation and corrosion are challenging issues in CO_2 EOR treatment (Wang et al. 2019). Furthermore, in tertiary oil production, many reservoirs are subjected to CO_2 flooding in which it contacts with the reservoir oil and changes the fluid properties and reservoir equilibrium conditions. It may lead to the precipitation of asphaltenes. Hence, one of the major challenges in the oil and gas industry during EOR treatment is related to asphaltenes precipitation.

Asphaltene deposition causes severe problems in the oil industry such as plugging the pores, altering the rock wettability, reducing the core permeability and subsequently decreasing the productivity rate (Kokal et al. 1992; Gabrienko et al. 2016). Asphaltenes deposition leads the production problems such as blocking the valves and submersible pumps (Leontaritis and Mansoori 1988). Mitigation of these problems is the goal of production engineers because the

remediation techniques are more expensive than its prevention. The treatment techniques for solving the formation damage problems causing by asphaltenes precipitation are slow, expensive, and hard to handle. Identifying the functional groups of asphaltene molecules is critical for the mitigation techniques of asphaltene precipitation. This thesis research aims to understand the changes in functional groups of asphaltenes in the presence and absence of carbon dioxide.

Srivastava et al. (1999) conducted the experimental analysis to indicate that the asphaltene precipitation in the single-phase region is increased linearly by CO_2 concentration. Carbonate reservoir oil in a PVT cell by using the light-scattering technique was studied by Takahashi et al. (2003). To find out the effect of CO_2 concentration on asphaltene precipitation, the pressure was gradually decreased at each predetermined CO_2 concentration and the results were compared. Based on their results, the precipitated asphaltene became considerable by exceeding the carbon dioxide concentration to more than 50 mol%. Furthermore, the asphaltene was precipitated due to CO_2 injection at the reservoir pressure.

Hu et al. (2004) studied the effects of pressure and injected CO_2 concentration on the asphaltenes precipitation under reservoir temperature. They concluded that the asphaltene was not precipitated under the pressure depletion process without CO_2 injection. But, when CO_2 was injected into the same system, the great amount of asphaltene was precipitated. There is a direct correlation between asphaltenes precipitation amount and injected CO_2 concentration.

The structure and molecular characteristics of four different asphaltenes were investigated by Ibrahim and Idem (2004) for determining the differences of inhibition effectiveness between CO_2 and n-heptane induced asphaltene precipitation. The results from FTIR and NMR tests

showed that the mechanism and behavior of asphaltenes precipitation is related to the oil and asphaltene characteristics, and asphaltene precipitant agent (that can be CO_2 or n-heptane). Furthermore, the type of inhibitor for asphaltene precipitation depends on the type of asphaltene precipitant and oil characteristics.

Okwen (2006) conducted a research on the chemical characteristics of formation water that influences on the rate or amount of CO_2 induced asphaltenes precipitation. CO_2 dissolves in the formation water and makes a buffer. Therefore, it is beneficial to identify the ideal formation water during the CO_2 injection. Minimizing the concentration of CO_2 injection to the reservoirs reduces the asphaltenes flocculation and precipitation. Core flooding and computer tomography (CT) scanning tests were also used to investigate the formation damage that is causing by the precipitation of asphaltenes during CO_2 flooding. It is very important to study the rock composition before CO_2 injection in EOR treatment.

Verdier et al. (2006) worked on the changes in asphaltene phase behavior by carbon dioxide injection. To do so, the high-pressure cell and a filtration technique were utilized. They found asphaltenes became more stable by increasing the pressure. However, for CO_2 injection, asphaltenes were more stable as the temperature decreased.

Zanganeh et al. (2012) visualized the asphaltene precipitation process by using a high-pressure cell and image processing technique. Their results show that CO_2 injection increases asphaltene precipitation in all pressure ranges. Moreover, increasing the mole percentage of CO_2 from 5 to 20%, rises the area of precipitated asphaltene and the differences in asphaltene molecular structures could be one of the main factors affecting asphaltene precipitation.

The asphaltene precipitation mechanism in the tight sandstone reservoir core plugs during immiscible, near-miscible, and miscible CO_2 flooding was studied by Cao and Gu (2013). The measured oil recovery factor (RF) shows that it increased by raising the pressure of immiscible CO_2 flooding. When the oil pressure exceeds the minimum miscibility pressure (MMP), the oil RF increases to reaches its highest value that is the maximum value in the miscible CO_2 flooding. Moreover, a higher average asphaltene content of the produced oil is found during the immiscible CO_2 injection conditions, whereas a lower average asphaltene content of the produced oil occurs under the miscible CO_2 flooding.

Dong et al. (2014) investigated the effect of temperature, pressure, and concentration of CO_2 on asphaltene precipitation. FTIR, interfacial tensiometer, and drill core displacement experimental apparatus were used in this experiment to determine the variation of the core oil permeability, and asphaltene content of produced oil by CO_2 flooding. By increasing the pressure of carbon dioxide and the molar ratio of CO_2 to oil and decreasing the temperature, the amount of precipitated asphaltene is increased due to the changes in interfacial tensions. These changes reduce the oil permeability that is related to blocking the pores by asphaltene precipitation.

Mohammed and Gadikota (2019) studied the effect of CO_2 injection on the structural properties of asphaltenes solvated in toluene in calcite nanopores by using molecular dynamics simulations. By increasing the CO_2 mole fraction, the van der Waals and electrostatic forces between the asphaltene and calcite surface are decreased. It also facilitates the asphaltene aggregation. In addition, CO_2 has a higher influence on asphaltene aggregation in the absence of confining solid interfaces.

Considering all the literature review, the impact of CO_2 on asphaltenes structure hasn't been studied completely by using the experimental techniques. Hence, my research area focuses on releasing the applicable and low-cost technique for finding the probable changes of asphaltenes structure during CO_2 flooding that is relevant in small laboratory scale running the test on a large scale in the industry.

Asphaltenes Precipitation Onset Point

One of the first steps to prevent asphaltene deposition is attaining the accurate information about the asphaltenes structure and its properties like stability. The stability of asphaltene is defined by measuring the onset of asphaltene precipitation, which means the minimum amount of precipitant that is required for precipitating the asphaltenes and the beginning point of separation of asphaltenes from oil. This point is obtained by monitoring the flocculating agent's volume that is essential for observing the first point of asphaltenes precipitation (Mansur et al. 2009). In this experiment, the onset of asphaltene precipitation was determined by ultraviolet-visible spectrophotometry (UV-Vis) and spectrofluorimetry for comparing the effect of stabilizers. Generally, spectrometer works based on comparing the quantity of light passes through the sample with the ones that pass through the reference (blank).

There are many methods and experimental techniques for determining the asphaltenes precipitation onset point to investigate its stability in crude oil. For instance, it can be found through detecting the accurate viscosity of oil that is diluted with a precipitant. It works based on an increase in the viscosity of the suspension of oil and precipitant, and comparison of the analyte curve with a reference system (Escobedo and Mansoori 1995). The capillary viscometer was used for measuring the viscosity. Moreover, the polyaromatic core of asphaltenes can strongly interact

with the external electric field. As a result, the electrical conductivity has appeared. Since the asphaltene precipitated from oil, the electrical conductivity changes abruptly. Therefore, it is one of the methods for finding the onset of asphaltenes precipitation point (Behar et al. 1998; Fotland et al. 1993).

Optical microscopy is another method that has been used to identify the precipitation of asphaltenes as a function of precipitant concentration. A series of oils and different n-alkane precipitants from n-pentane through n-pentadecane were prepared in a certain volume. After reaching the equilibrium, the optical microscope at a magnification of 320× was used for finding the onset of asphaltenes precipitation (Wang and Buckley 2003). However, the optical microscopy technique is not so accurate. Since ultra-heavy crude oils are so viscous, a laser with near-infrared wavelength cannot penetrate them.

Wattana et al. (2003) utilized the refractive index of crude oils to understand their tendency to precipitate from crude oils. First, different crude oils were titrated by heptane or pentane to induce asphaltenes precipitation. Then the refractive index of these solutions was measured. At the beginning of the measurement, it is the linear combination of refractive indexes of the components of oils. When asphaltene starts precipitating from oil, the refractive index has slightly deviated from the linear line. In this experiment, the careful analysis of refractive indexes is required to see the small deviation from the linear line.

Gharfeh et al. (2004) presented the near-infrared (NIR) light transmittance technique for detecting the onset of asphaltenes precipitation of crude oils. The system contains a titration vessel, a temperature controller, an automatic titrator, a NIR laser set, and a transmittance detector. A

sample was titrated continuously at a rate of 1 mL/min with heptane. Then, the transmittance was plotted as a function of the titrant volume or time. The apex of this plot is the onset point for asphaltenes precipitation. This method is also applicable to ultra-heavy oil cases. On the other hand, Mousavi-Dehghani et al. (2004) conducted research on finding the asphaltene precipitation onset point based on the measuring the interfacial tension (IFT) between oil and water phases that the sudden changes in the IFT show the onset point. First, the crude oils were mixed with n-heptane. Then, the IFT between the water and this solution was measured by the DuNouy ring method.

The direct methods for measuring the precipitation onset point can detect the presence of asphaltenes particle with a minimum size of 0.5 to 1 μm. It means that the direct methods such as optical microscopy and NIR scattering determine the onset point when the aggregation of precipitated asphaltenes exceeds this particle size. These methods couldn't detect the precipitation amount. They just identify the particles with a specific size, not their quantities. Alboudwarej et al. (2005) utilized the indirect procedure for detecting the asphaltenes concentration adsorbed on the solid metal surface by using the UV-Vis spectrophotometry. In this research, the differences between initial and final asphaltene concentrations reveal the number of deposited asphaltenes on the metal surface. This work motivated other researchers to use the indirect method for finding the onset of asphaltenes precipitation.

Tavakkoli et al. (2015) prepared samples containing different ratios of n-heptane and oil. UV-Vis spectrophotometer was used to detect the onset point and quantify the number of precipitated asphaltenes. This indirect method can be used for various crude oil types with different asphaltenes concentration. Furthermore, this method is very sensitive to the asphaltene particle

size that is precipitated and the minimum detectable particle size of asphaltene is smaller than the previous direct methods. Therefore, with this literature review, for quantifying the amount of asphaltenes precipitation, its stability is measured by the UV-Vis test in the presence of n-alkane and carbon dioxide separately to distinguish the effect of precipitant on its precipitation onset point.

Research Objectives

The propensity of the asphaltene molecule toward precipitation is associated with its structure (Borton et al. 2010), but the exact composition and chemical structure of asphaltenes are still unknown. It is obscure that the precipitation of asphaltene by CO_2 is coming from structural changes or not. So, it is beneficial to understand how amplifier factors will precipitate the asphaltenes.

The current study identifies the relationship between the asphaltenes composition and its stability under CO_2 flooding. The influences of CO_2 on asphaltenes structure has not been studied thoroughly. Since the main purpose of this work is to present the valid techniques for determining the probable changes in the structure of asphaltenes under CO_2 injection and its effects on the onset of asphaltenes precipitation. Another important interest in this work is to specify which new functional group in CO_2-reacted asphaltene has a direct impact on its instability.

CHAPTER II

EXPERIMENTAL METHODOLOGY*

The objective of experimental work is evaluating the probability of asphaltene structural changes due to carbon dioxide injection and understanding how these changes affect asphaltene stability in the crude oil system. These will be experimentally conducted by fourier transform infrared and ultraviolet-visible spectroscopy.

Materials

Four different light, medium, and heavy crude oils from different regions (A from China, B from the Gulf of Mexico, C from Alaska, and D from west Texas) were studied in the present work. Normal heptane (≥99 wt.%, HPLC Grade), and toluene (99.8 wt.%, HPLC Grade) from Alfa Aesar were used as an asphaltenes precipitant and solvent, respectively. 1,4-diazabicyclo[2.2.2]octane (DABCO) base was obtained from Alfa Aesar with 98% purity. The function of this base is collapsing the H-bonded ion pair that existed in the asphaltenes structure. In other words, it can capture asphaltenes acidic hydrogens. The structure of this base is shown in **Figure 2**. Hydrochloric acid will be used to determine the functional group generated by carbon dioxide in the identification test. It was obtained from Macron and was titrated against a 1N sodium

* Part of this chapter is reprinted with permission from "Asphaltene Structural Changes Induced by Carbon Dioxide Injection" by Golshahi, N., Afra, A., Samouei, H., Nasr-El-Din, H. 2019 OTC Offshore Technology Conference Brasil, OTC-29730-MS. Copyright 2019, Offshore Technology Conference.

hydroxide solution and found to have a concentration of 36.8 wt.%. Acetone (Semiconductor Grade, 99.5%) will also be used for resin separation from Alfa Aesar.

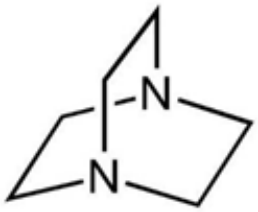

Figure 2. Chemical Structure of the DABCO Base.

SARA Analysis

SARA analysis experiment was conducted to determine the composition of oil samples based on their solubility in solvents of diverse polarity and affinity for absorption to solid granular packing columns such as silica gel, alumina, and natural clays. In this method, the oil samples are classified into saturates, aromatics, resins, and asphaltenes based on the American Society for Testing and Materials (ASTM) standard D2007-11. **Figure 3** shows the SARA analysis separation. Asphaltenes from four different crude oils were precipitated by adding n-heptane in a ratio of 1:40 oil to n-heptane (Goual and Firoozabadi 2002). n-Heptane is chosen to preserve the light fractions of oil. The beaker containing mixtures of n-heptane and crude oils were stirred for 12 hours at 86°F on hotplate stirrer for n-heptane evaporation. The mixture was poured into a flask through a funnel with a filter paper. Then, they were allowed to rest for 2 hours. This process caused the precipitation of aggregation particles of asphaltenes that were left in filter paper. After vacuum filtration and air drying, the asphaltenes were collected and weighted.

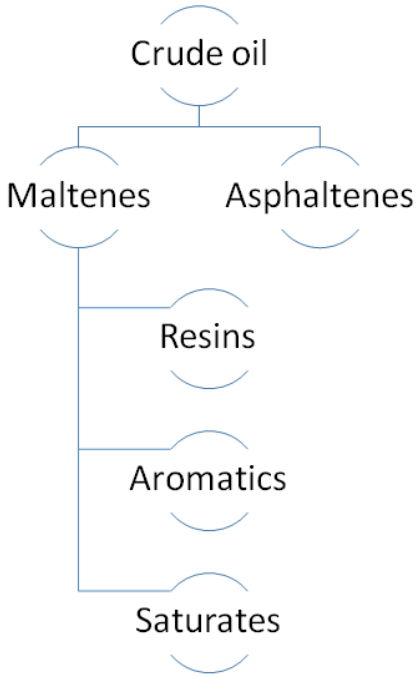

Figure 3. SARA Analysis Separation.

After asphaltene precipitation, the fraction that remains dissolved named maltenes. The adsorption columns needed for separating the saturates, aromatics and resins from maltenes. The maltenes passed through the clay-packed column and an activated silica-gel column, to adsorb resins and aromatics, respectively. For resins separation, a 50-50 volume mixture of toluene-acetone is charged through the column. The solution is passed through a filter paper and collected in a flask. n-Heptane is used to wash the funnel and filter paper and remove traces of the oil sample. The solution is evaporated at 86°F in a hotplate stirrer to remove the toluene, acetone, and n-heptane. Therefore, the resin is collected and weighted. For aromatics determination, Soxhlet extraction of the silica gel in toluene is utilized for recovering the aromatics fraction. Saturate is the remaining part and it is the last component of SARA analysis. The scheme of the SARA separation method is illustrated in **Figure 4** (Rakhmatullin et al. 2018).

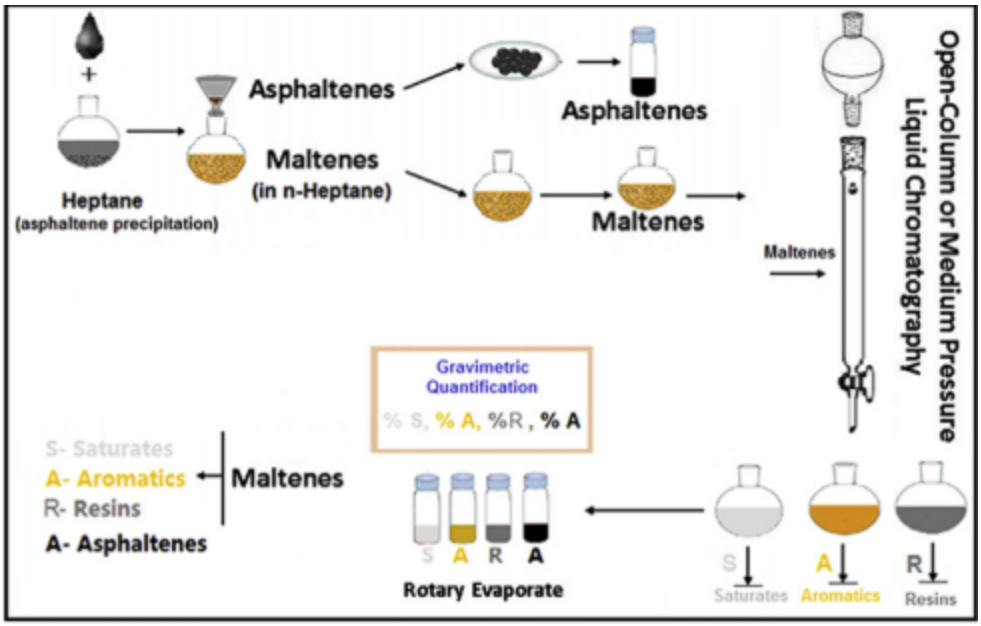

Figure 4. Scheme of SARA Analysis.

Elemental (C, H, N, S) Analysis

The elemental analysis includes the identification and determination of the elemental composition of materials such as carbon, hydrogen, nitrogen, and sulfur elemental content in various concentrations in samples with high accuracy. All of the elemental analysis methods are based on mass weighting. It means samples are weighted by calibrated balances. Elemental analysis divided into qualitative and quantitative methods. Qualitative methods help to find which elements are present in the samples. Whereas, the quantitative method determines the amount and percentage of each element in samples. This method couldn't determine the functional groups or structure. It can be performed on a solid, liquid, or gas depending on the samples.

In C, H, N and S elemental analysis, the sample is combusted in a pure oxygen environment by oxygen flask based on the ASTM D5622. The gases are converted to CO_2, H_2O, N_2, and SO_2 and carried out by helium. These gases are separated under steady-state conditions. Then, they are

detected by Infrared Spectroscopy (IR). Based on ASTM D5622, to find the organic oxygen percentage the sample is pyrolyzed. After the filtration of acid gases, the IR spectroscopy is used for organic oxygen detection. Furthermore, ion chromatography is used for the determination of halogen percentages (F, Cl, Br and I%). Oxygen flask combustion converts the halogens of samples to their ionic forms, such as bromide and chloride. After dilution and filtration, the percentages are calculated.

The Perkin-Elmer 2400 analyzer was used for determining the C, H, N and S contents of asphaltenes. This device is shown in **Figure 5**. The oxygen percentage can be calculated by difference. 1 mg of sample is grounded and then sieved to less than 0.2 mm (Leyva et al. 2013). The elemental analyzer software calculates the amounts of the gases as a percentage of the initial sample weight. Finally, C%, H%, N%, and S% are shown.

Figure 5. Perkin-Elmer 2400 C, H, N, S Analyzer.

X-ray Fluorescence (XRF)

The X-ray can be defined as electromagnetic waves with their wavelengths, or beams of photons with their energies. When X-rays contact the matter, three main interactions would happen: Fluorescence, Compton scatters and Rayleigh scatters (Brouwer 2006). These interactions are shown in **Figure 6**. A fraction of the beam of X-ray photons can be adsorbed and produced fluorescent radiation or scattered. Scattering with a loss of energy is Compton scatter. On the other hand, Rayleigh scatter is the one without loss of energy. The scatter or fluorescence depends on density (ρ), thickness (d), the composition of the material, and energy of the X-rays.

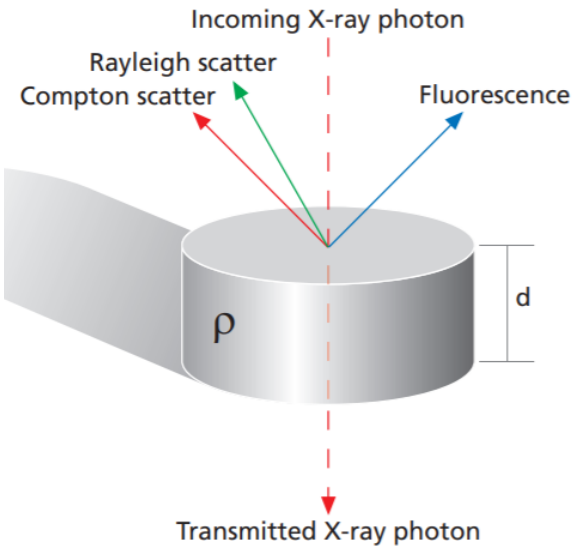

Figure 6. Three Main Interactions of X-Rays with Matter.

X-ray Fluorescence (XRF) is one of the broad application elemental analysis techniques in science and industry. Since, it is the nondestructive elemental analysis method for solids and liquids, powders, and other forms. This method is fast, easy, accurate and requires a minimum of

sample preparation. The analysis time varies between seconds and 30 minutes based on the number of elements. The analysis time after the measurement is only a few seconds.

XRF spectrometer contains a source, a sample, and a detection system. The sample was irradiated by the X-ray beam that is produced by the source. X-ray tube (that is shown in **Figure 7**) is often used as a source. It contains a filament (wire) and an anode. The anode is placed in the vacuum housing. Electrons are emitted by heating the filaments. A high voltage is applied to the filament and anode. This high voltage accelerates the electrons toward the anodes. They are accelerated towards a metal target at energies of several thousand electron volts. When these electrons hit the metal target, X-rays are produced. Therefore, X-rays are generated inside the tube by free electrons. The X-rays emitted from the sample show the interactions of electrons inside the matter. Hence, by measuring the energies of X-rays that are emitted from a matter and counting the number of X-rays of each energy, XRF is practical in identifying the type of elements inside different samples, and relative concentration of them.

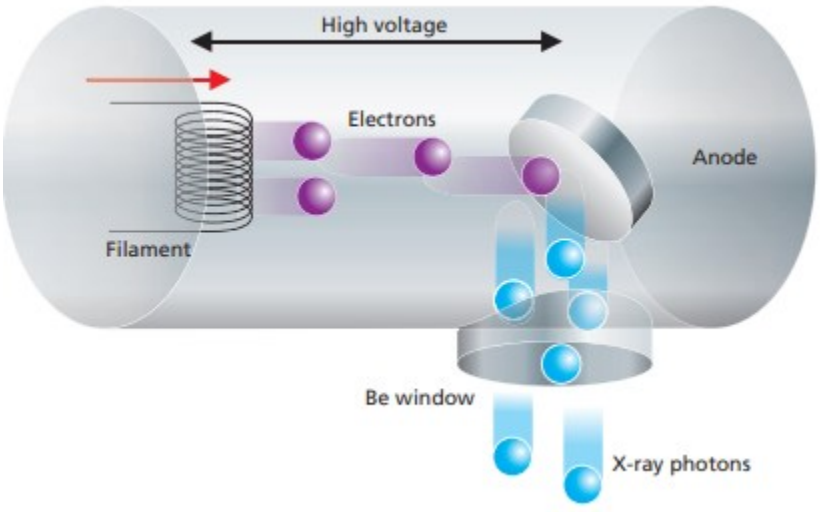

Figure 7. Design of the X-Ray Tube.

The emitted X-rays can be detected by using energy or wavelength dispersive detector. Therefore, the elements present in the sample are detected by the energies or wavelengths of the emitted X-rays and their concentrations are determined by the intensity of the X-rays. Generally, spectrometers are divided into energy dispersive systems (EDXRF) and wavelength dispersive systems (WDXRF). Detectors of EDXRF measure the energies of radiation that is emitted from the sample. Then, the radiation from the sample is separated into the radiations from the elements inside the sample. This separation is called dispersion. Solid-state detectors are mainly used in EDXRF. This wide range of detectors measures all elements from sodium (Na) to uranium (U). In WDXRF spectrometers, the analyzing crystal is used to disperse the different energies of radiation that is coming from the sample. The detectors used in this spectrometer are gas-filled detectors that measure elements from beryllium (Be) up to copper (Cu), and scintillation detectors that quantify elements from Cu up to U. The resolution of these two detectors are poor. So, they are suitable for wavelength dispersive spectrometers in which the resolution is enhanced by the crystal.

Since XRF is a sensitive technique, the samples should be completely clean without the sign of fingerprint. The sample is placed in a cup, and the cup is placed in the spectrometer. Most XRF spectrometers are designed to measure samples with a radius between 5 and 50 mm. It is required to clean and polish the solid samples. Liquids are poured into cups that contain supporting films. For obtaining sufficient liquids, diluents should be added. In this experiment, the XRF analysis was taken from the solution of asphaltenes and toluene for finding the elements and their concentrations in asphaltenes samples.

CO_2 Injection

To identify the probable changes in asphaltene structure during CO_2 flooding, carbon dioxide should be injected into model oils. The model oil is the solution of 200 mg of asphaltenes and 5 ml of toluene. **Figure 8** shows the pressurized reactor that was used in this experiment. The initial pressure of CO_2 was 870 psi. Afterward, the pressurized reactor was placed on hot plate stirrer (752°F) for 3 days. Due to providing the small scale of downstream in petroleum labs, this T and P were selected. The magnetic stirrer should be used in the reactor for circulating the CO_2 and solution constantly. Otherwise, CO_2 may place at top of the reactor and don't have a chemical reaction with oil. The experiment was repeated for 7 days to determine the effect of CO_2 injection time on asphaltenes structure. Due to the dispersion of the negligible amount of CO_2-reacted asphaltenes, they could not be collected and measured from the reactor entirely after the experiment. Carbon dioxide (with the same pressure and temperature) was injected into four different crude oils directly. After running the same experiment, n-heptane was added to these oils for precipitating the asphaltene, in which the n-heptane volume was 40 times more than the oil volume.

Figure 8. Reactor Used in Experiments.

Fourier Transform Infrared Spectroscopy (FTIR)

FTIR method can help us to characterize the samples, identify unknown materials, and determine the amount and quality of components in a mixture. The light used in this spectroscopy is electromagnetic radiation that is composed of electric and magnetic waves called the electric vector and the magnetic vector. These two waves go through the cycle because their motions are repetitive. One cycle is terminated when a wave has crossed zero amplitude a third time as illustrated in **Figure 9**. Wavelength is the distance between two identical adjacent points in a wave. Another light property is wavenumber that defines by the number of waves in a unit distance. Wavenumber and wavelength are reciprocals of each other where W is wavenumber and λ is the wavelength.

$$W = 1/\lambda \quad (1)$$

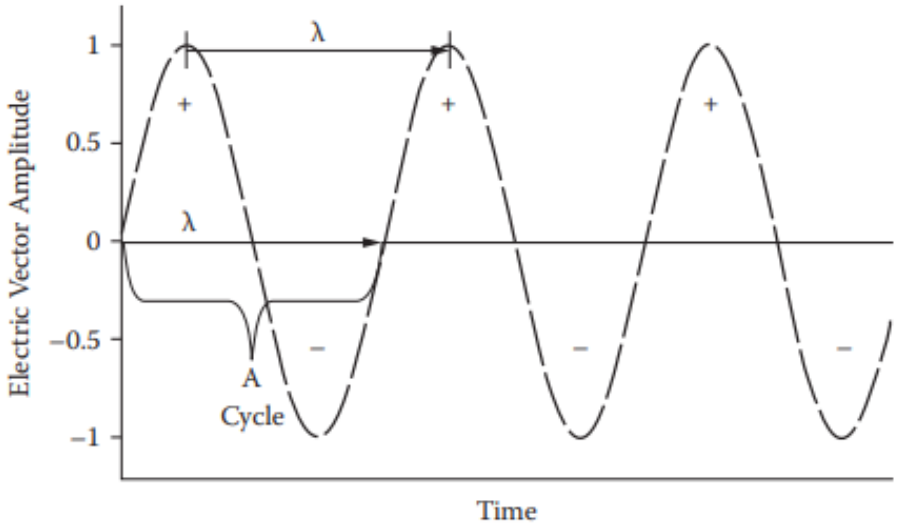

Figure 9. An Example of a Wave's Cycle and Wavelength.

In this technique, the absorbed and transmitted radiations from a sample are collected and used to generate a spectrum of a sample. FTIR spectrum is a plot of infrared light intensity as a function of wavenumber (cm^{-1}) which means how much light a sample can be adsorbed. The absorbance spectrum of a sample is calculated by:

$$A = \log(I_0/I) \tag{2}$$

Where A = Absorbance, I_0 = Intensity in the background spectrum, and I = Intensity in the sample spectrum. Percent transmittance measures the percentage of light transmitted by a sample that is calculated from the following equation:

$$T\% = 100 \times (I/I_0) \tag{3}$$

Where T% is the percent transmittance. FTIR software can easily convert the absorbance to the percent transmittance. Because these two terms are mathematically related to each other. This change does not affect the peak positions.

Infrared spectra used to identify the type of the molecules and functional groups presenting in the sample. One of the unique physical properties of the molecule is a vibrational spectrum that

works as a fingerprint for sample characterization. Therefore, the FTIR spectra of the solutions were taken by the transmittance percentage as a function of wavenumber (cm^{-1}) on the Thermo Nicolet 380 FTIR spectrometer that is shown in **Figure 10**. The FTIR spectra were collected in the wavenumber region of 4000-400 cm^{-1} at 4 cm^{-1} resolution (Król et al. 2016).

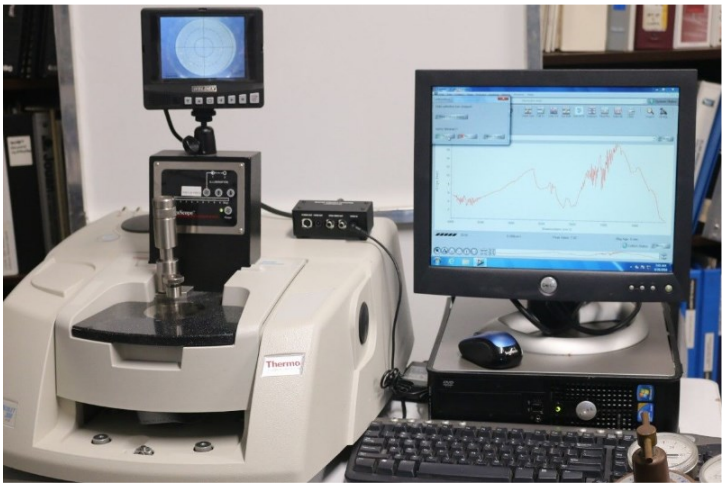

Figure 10. Thermo Nicolet 380 FTIR Spectrometer.

The instrumental components of FTIR are as follows:

1) Source: the source emits the infrared energy as a beam that passes through the interferometer and sample simultaneously to control the amount of energy presented in the sample. 2) Interferometer: the beams from the source enter the interferometer to create an interference pattern, which can be measured and analyzed. It works by merging different beams. 3) Sample: by entering the beam into the sample, it can be transmitted, absorbed or reflected off the sample's surface (based on the characterization of the sample). 4) Detector: then, the beam passes through the detector that is used to measure specific signals for identifying the unknown components of the sample. 5) Computer: The measured signal is digitized and sent to the computer where the fourier

transformation takes place. Then, the final spectrum is presented to the user for further interpretation. **Figure 11** shows the components of the FTIR spectrometer.

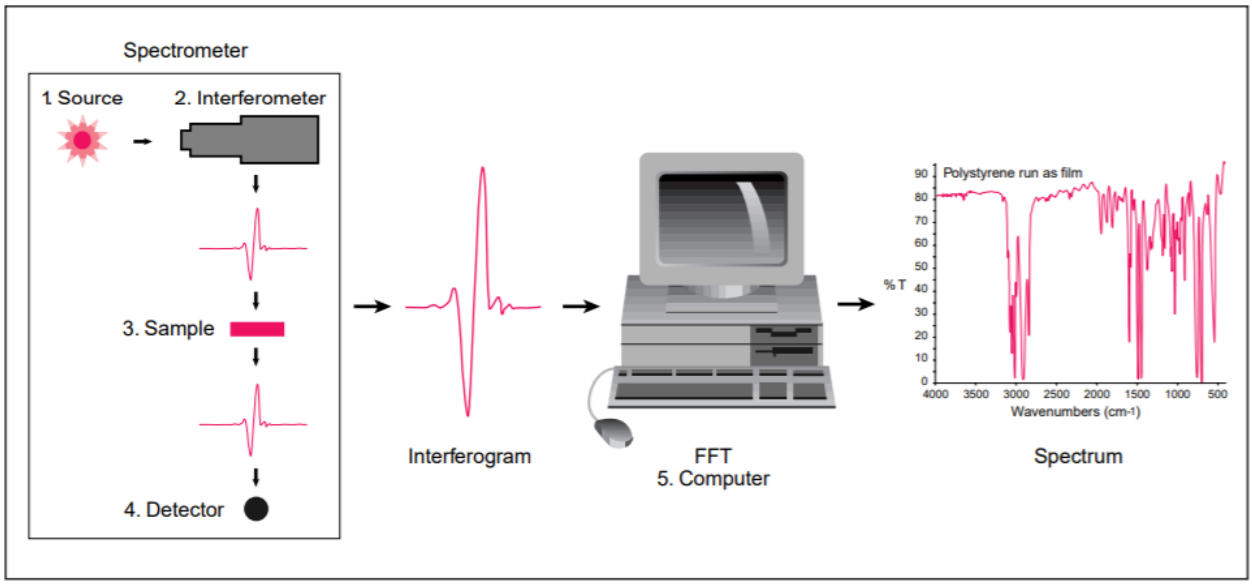

Figure 11. Components of the FTIR Spectrometer.

The FTIR method has some advantages over the previous methods such as its speed and sensitivity. All the signals are measured simultaneously and running the FTIR test on a sample takes less than a minute. Furthermore, FTIR is a very sensitive method. Because the detectors used have high sensitivity. Hence, the results have much lower noise levels compared to the previous methods. For avoiding the probable noises, the background spectrum must be measured when there is no sample in the beam. Another advantage of FTIR is internally calibrated. It means that the instrument is self-calibrating and never needs to be calibrated by the user.

Samples may be in liquid, solid or gaseous form. In this experiment, to obtain high precision dried solid samples of asphaltenes were used. In this spectrometer, the analysis area can

be as small as 10 μm. The FTIR results of asphaltenes were compared before and after CO_2 injection to identify the possible changes in its structure by carbon dioxide.

Identification Tests

To determine and characterize the functional groups generated by carbon dioxide and their formation mechanism, two identification tests were conducted. The first test consisted of mixing 100 mg of DABCO with 200 mg of asphaltenes that were diluted in 3.5 ml toluene. Then, the solution was pressurized with CO_2 at 752°F for 2 days and its FTIR spectrum was collected. In addition, the same experiment was repeated for the solution of 7 g of oil and 100 mg of DABCO base as a control experiment. Next, its asphaltene was precipitated by n-heptane. Most of the common bases can react with CO_2 and generate new functional groups, however, the DABCO base that is selected for this experiment does not have any chemical reaction with CO_2. The function of this base is collapsing the H-bonded ion pair that existed in the asphaltenes structure (Cecchi et al. 2006). In other words, it can capture asphaltenes acidic hydrogens. This experiment is conducted to identify the existence of any hydroxyl groups in CO_2-reacted asphaltenes and to determine the functional group that detected the carbonyl group belongs to.

Analysis of asphaltenes structural changes can be done by the hydrolysis and degradation reaction of the amide group in the presence of HCl that is shown in **Figure 12** (O'Connor 1970). This reaction shows that the amide hydrolysis generates carboxylic acid and amine groups. Therefore, the second identification test was done by mixing 100 mg of CO_2-reacted asphaltenes with 5 ml of hydrochloric acid and 2 ml of water. Then, the solution was heated for 30 min at 140°F. After drying, the FTIR spectrum of this sample was taken.

Figure 12. Reaction of the Amide with Water in the Presence of Hydrochloric Acid for Producing a Carboxylic Acid.

Control Test

To examine whether the changes in the structure of asphaltenes were due to carbon dioxide injection, nitrogen gas (870 psi) was also injected to the solution of 200 mg asphaltenes and 5 ml toluene. The solution containing N_2 gas was stirred at 752°F for 7 days. Then, the FTIR test was taken from these asphaltenes. Since N_2 gas is neutral and doesn't have any chemical reaction with the crude oil, it was selected for this control experiment.

UV-Visible Spectroscopy

Several different processes can occur when radiation interacts with the surface. They can be the reflection, scattering, absorbance, fluorescence and photochemical reaction (absorbance and bond breaking). The absorbance is just considered in UV-Visible spectra. The absorbance of light by a compound can increase the energy level of molecules. Because light is a form of energy. The total potential energy of a molecule equals the summation of electronic, vibrational, rotational and translational energies.

$$Etotal = Eelectronic + Evibrational + Erotational + Etranslational \quad (4)$$

Translational energy relates to the displacement of molecules in space as a function of the thermal motions of matter but the rotational energy refers to the tumbling motion of a molecule as a result of the absorption of energy within the microwave region. Furthermore, the vibrational energy relates to the absorption of energy by a molecule that is vibrated about the mean center of their chemical bonds. Eventually, electronic energy is the transition energy of electrons when they are distributed throughout the molecule. It may happen in some molecules and atoms that the photons of UV and visible light have enough energy to cause transitions between the different electronic energy levels. This energy is enough to move an electron from a lower energy level to a higher energy level.

A spectrophotometer is an instrument for measuring the transmittance or absorbance of a sample as a function of the wavelength of radiation. The components of a spectrophotometer are a source, dispersion device, sample, detector, lenses, and mirrors. Two sources are used in UV-Vis spectrophotometers including deuterium arc lamp and tungsten-halogen lamp. The deuterium arc lamp yields good intensity in the visible region with very low noise. The intensity of light decreases steadily in time. The tungsten-halogen lamp provides a useful intensity over part of the UV spectrum. It has a very low noise like the other lamp. Finally, the light from two sources is mixed to make a broad single source. The dispersion devices are used to disperse the light from different angles. Prisms and holographic gratings are the two common dispersion devices in UV-Vis spectrophotometers. Prisms are inexpensive dispersion device that generates rainbow from sunlight. But the dispersion angle is sensitive to temperature. Therefore, the recent spectrophotometers contain holographic gratings instead of prisms. These are made of glass blanks with an aluminum coating to reflect the light at diverse angles. A detector converts a light signal

to an electrical one. The response should be linear with high sensitivity and low noise. Detectors used in UV-Visible spectrophotometer are photomultiplier tube detector or a photodiode detector. The photomultiplier tube contains cathode and anode part that combines signal conversion with several stages of amplification. This detector provides high sensitivity at a low level of light while the ideal detector must have low noise at high-intensity levels to distinguish the small differences between the blank and sample measurements. Thus, the photodiode detector is recently used as a detector. It has a litter wide dynamic range. In this detector, when light falls on the material, it allows an electron to flow in it and depletes the charge in a capacitor. The amount of charge for recharging the capacitor is proportional to the light intensity. In some modern spectrophotometers, an array of photodiode detectors is used instead of one.

The cells that are used in the UV-Vis spectrometer, must be transparent at all wavelengths. Fused quartz cells should be beneficial up to 210 nm and fused synthetic silica cells are transparent down to 190 nm. The ideal solvent for sample preparation would dissolve all kinds of compounds and be transparent to all wavelengths.

Only a few broad absorbance bands are seen in UV-Vis spectra. Therefore, it can provide a limited amount of qualitative analysis results compared with the FTIR spectra and they are not able to identify the unknown compounds. But they are used to confirm the identity of a matter by comparing the measured spectrum with a reference one.

Asphaltenes Precipitation Onset Point

Stabilities of asphaltenes samples were evaluated through the measuring of precipitation onset point following the method proposed by Tavakkoli et al. (2015). The toluene was added to

the proper amount of asphaltenes to prepare the 0.5 wt.% model oil. To avoid any undissolved sediment particles in the mixture, the solution was stirred continuously for 30 minutes at 180°F and then sonicating it for 15 minutes at 50 kHz. After centrifugation, no undissolved particles were observed. The 0.5 wt.% was selected for a concentration of model oil to represent a low asphaltene concentration and avoid asphaltene deposition problems. Therefore, it is arbitrary. Then n-heptane was added at the rate of 1 ml/min in the concentration range of 10 to 90 vol% to induce asphaltenes precipitation. So, samples containing different ratios of model oil and n-heptane were prepared. The test tubes were shaken by hand and placed on the untouched surface for a couple of minutes. Next, the test tubes were centrifuged for 2 hours at 10,000 rpm to remove the unstable asphaltene particles. 1 ml of the supernatant of each solution was taken and diluted with 4 ml of toluene. Then, the absorbance of samples as a function of wavelength was measured by the Shimadzu UV 2501PC spectrophotometer that is shown in **Figure 13**.

Figure 13. Shimadzu UV 2501PC Spectrophotometer.

The dilution effect should be removed from the measured absorbance and the plot of absorbance vs n-heptane volume fraction was obtained. The sharp deviation of the linear line of the plot shows the onset point of asphaltene precipitation. This experiment was conducted to identify the relation of asphaltene structural changes by CO_2 flooding and its stability alteration.

To better identify the onset point, the absorbance at 350 nm was plotted as a function of n-heptane vol%. Because the changes in absorbance of samples at 350 nm were greater compared to the other wavelengths. So, 350 nm was selected. But, the absorbance at different wavelengths can be selected and this method works for any wavelengths.

CHAPTER III

RESULTS AND DISCUSSION[†]

Oil Characterization

SARA Analysis

Table 1 shows the SARA fractions of four tested crude oils. Various types of crude oils in terms of asphaltenes fraction and API gravity were investigated in the present study using the ASTM D2007-11. Also, these samples are different regarding asphaltenes associated problems and its percentage in the oil. For instance, although sample **D** has the lowest amount of asphaltenes, it has severe asphaltenes precipitation and deposition problems during production (Afra et al. 2017). There is not a logical correlation between the asphaltenes amount and its problem severity in the oil and gas industry.

Table 1. Oil Samples Characterization.

Oil Sample	Type	Saturates (wt.%)	Aromatics (wt.%)	Resins (wt.%)	Asphaltenes (wt.%)
A	Heavy	31	26	15.7	27.3
B	Heavy	20.6	24.5	19.1	35.8
C	Medium	43	30	11	16
D	Light	48	43	5	4

[†] Part of this chapter is reprinted with permission from "Asphaltene Structural Changes Induced by Carbon Dioxide Injection" by Golshahi, N., Afra, A., Samouei, H., Nasr-El-Din, H. 2019 OTC Offshore Technology Conference Brasil, OTC-29730-MS. Copyright 2019, Offshore Technology Conference.

Asphaltenes Characterization

Elemental (C, H, N, S) Analysis

Table 2 presents the elemental analysis results of asphaltenes. The hydrogen to carbon ratio (H/C) was used to find the level of asphaltenes aromaticity. The higher H/C ratio represents the lower aromaticity (Marcano et al. 2011).

Table 2. Elemental Analysis of Asphaltenes.

Asphaltene	A	B
Carbon (wt.%)	**87.48**	**82.03**
Hydrogen (wt.%)	**7.50**	**7.87**
Nitrogen (wt.%)	**1.32**	**0.68**
Sulfur (wt.%)	**2.77**	**2.24**

The ratio between hydrogen, carbon, nitrogen, and sulfur atoms are presented in **Table 3**. It indicates that due to the higher H/C atomic ratio, asphaltenes **B** are less aromatic than **A**. It concluded that the asphaltenes **B** contain longer aliphatic chains and lower content of heteroatoms (N and S) than asphaltenes **A**. The heteroatoms are more commonly found in the aromatic rings. Hence higher S/C ratio indicates the heavier oil with a higher proportion of heteroatoms in the asphaltenes.

Table 3. Atomic Ratios of Asphaltenes.

Asphaltene	A	B
H/C	**0.086**	**0.096**
S/C	**0.032**	**0.027**
N/C	**0.015**	**0.0082**

X-ray Fluorescence (XRF)

The type and concentration of different elements of asphaltenes **A** and **B** are shown in **Tables 4** and **5** respectively. Asphaltene **A** contains a great amount of vanadium (V). Whereas, high concentration of manganese (Mn) and calcium (Ca) are present in asphaltene **B**.

Table 4. XRF Results of Asphaltenes A.

Formula	Z	Concentration
V	23	0.141
P	15	0.0772
Ni	28	0.0332
Ca	20	0.0318
Fe	26	0.0072
K	19	0.0069
Nd	60	0.0043
Si	14	0.004
Ti	22	0.002
Cu	29	0.002

Table 5. XRF Results of Asphaltenes B.

Formula	Z	Concentration
Mn	25	0.615
Ca	20	0.122
P	15	0.0578
K	19	0.0169
Fe	26	0.0157
V	23	0.0058
Sr	38	0.0031
Zn	30	0.0009
Cu	29	0.0007
Rb	37	0.0005
Ni	28	0.0005
As	33	0.0003
Pb	82	0.0003

Effect of CO_2 Injection on Asphaltenes FTIR Spectra

FTIR spectroscopy was conducted to investigate the existence of a correlation between asphaltenes functional groups and their properties such as solubility and stability. To do so, the FTIR spectrums of asphaltenes samples before and after reaction with CO_2 were compared to detect the differences in the intensity and type of functional groups. **Figure 14** shows the FTIR spectrums of asphaltenes **A**.

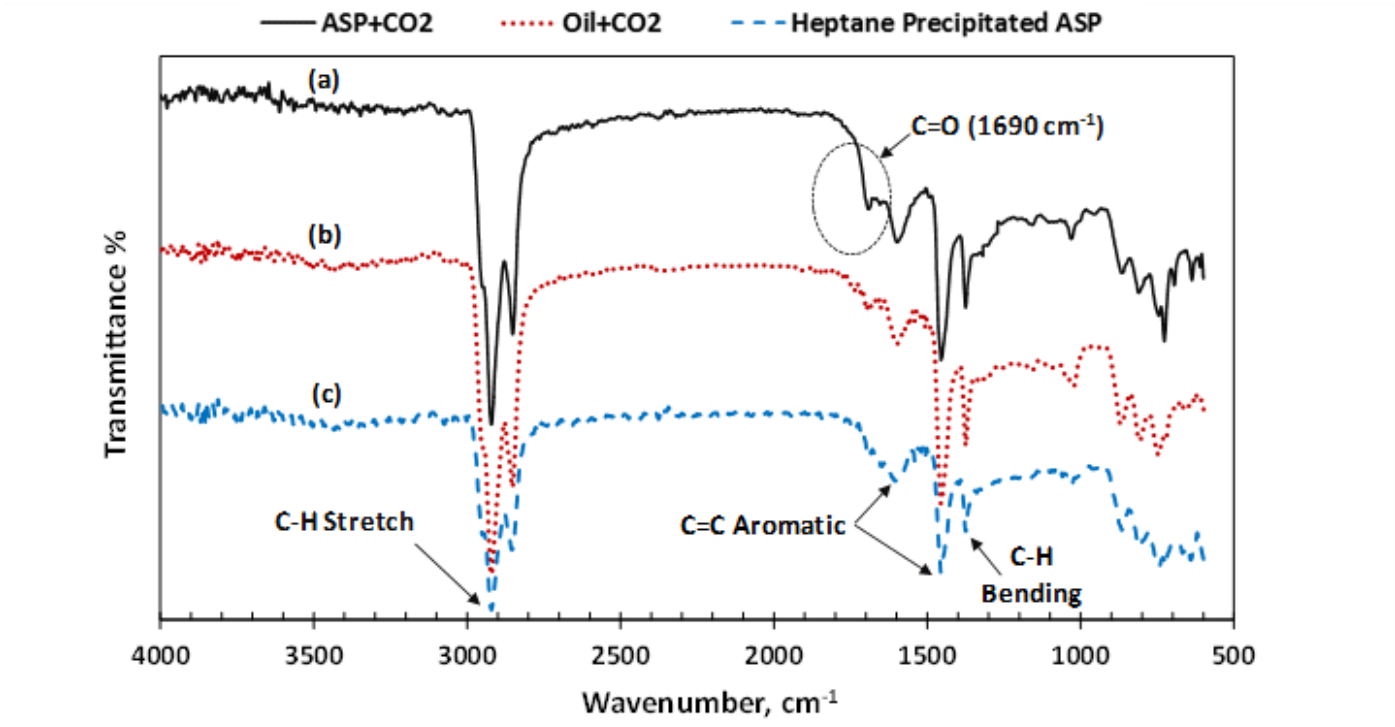

Figure 14. FTIR Spectra of (A) the Asphaltenes A in Which CO_2 Was Injected to the Asphaltenes for 3 Days, (B) the Asphaltenes That Were Precipitated from Crude Oil A in Which CO_2 Was Injected to the Oil for 7 Days, and (C) the Asphaltenes A without CO_2 Injection.

Two peaks of 1600 and 1475 cm^{-1} are indicating the C=C aromatic bonds. The peaks indicating the CH stretching and bending are located at 2800-2990 cm^{-1} and 1405 cm^{-1} respectively. In addition, the FTIR spectrum in the region of 2800-3000 cm^{-1} is representative of the carbon-

hydrogen stretching vibrations. These results also stipulated that after a reaction time of 3 days, a new peak at 1690 cm^{-1} was formed in the presence of CO_2. The band at around 1700 cm^{-1} can be attributed to the carbon-oxygen double bond (Pavia et al. 2008). Therefore, this peak could be associated with different carbonyl functional groups. Further experimental results on the characterization of this functional group will be discussed later in the thesis. These results prove that carbon dioxide can react with asphaltenes **A** and produce a new functional group.

To understand the influences of a duration of the CO_2 reaction experiments on the asphaltenes compositional change, carbon dioxide was injected into the solution of asphaltenes **A** and toluene for 3 and 7 days and their FTIR spectrums were collected (**Figure 15**).

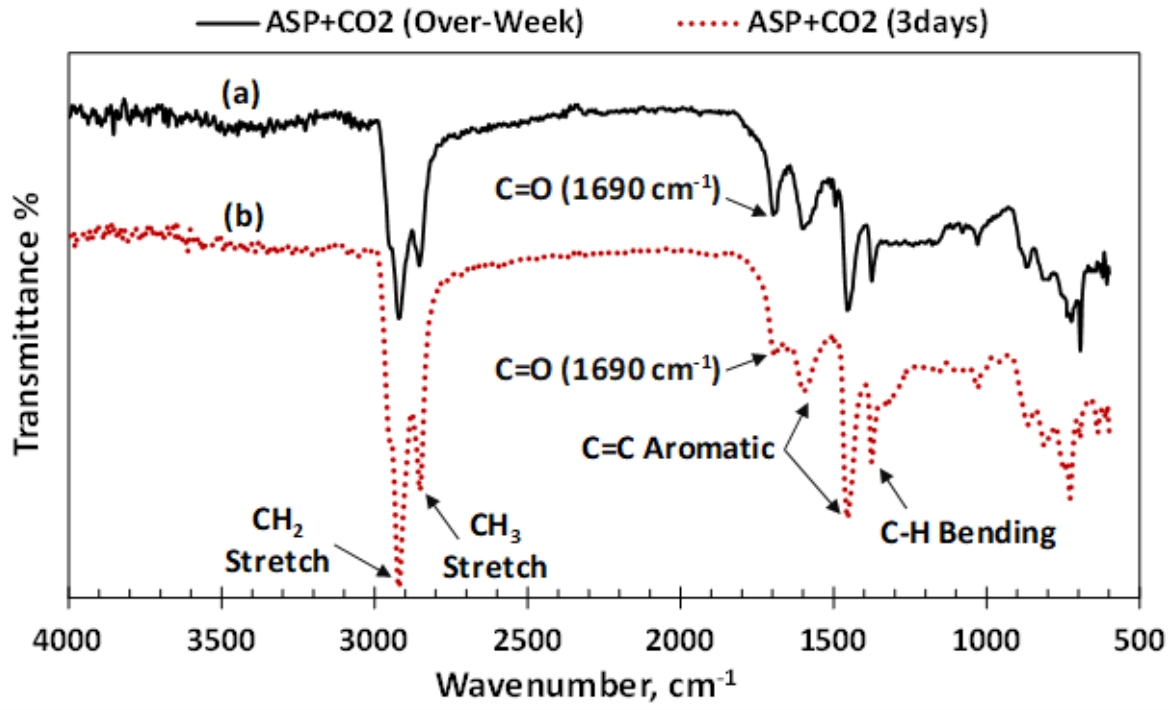

Figure 15. FTIR Spectra of the Asphaltenes A in Which CO_2 Was Injected to the Asphaltenes for (A) 7 Days and (B) 3 Days.

The results showed that the 1690 cm^{-1} band became significantly stronger in the sample reacted with CO_2 for 7 days compared to the sample with 3 days reaction time. Therefore, experimental time plays an important role in completing the reaction of CO_2 and asphaltenes. The generated new signal bond at 1690 cm^{-1} was intensified by increasing the CO_2 injection time from 3 to 7 days and the new functional group was formed by increasing the duration of the experiments.

Figures 16 through **18** shows the FTIR spectrums of samples **B**, **C**, and **D** before and after reaction with CO_2. These results demonstrate no significant differences between asphaltenes spectrums before and after a one-week CO_2 injection.

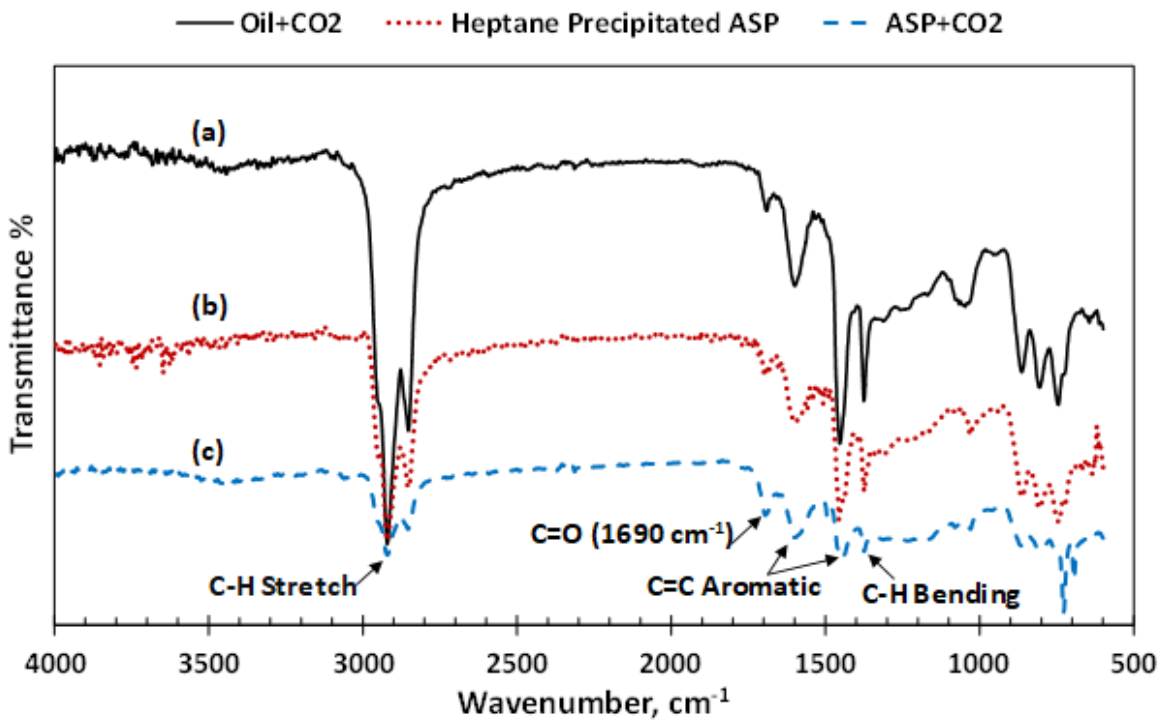

Figure 16. FTIR Spectra of (A) the Asphaltenes That Were Precipitated from Crude Oil B in Which CO_2 Was Injected to the Oil for 7 Days, (B) the Asphaltenes B without CO_2 Injection, and (C) the Asphaltenes B in Which CO_2 Was Injected to the Asphaltenes for 7 Days.

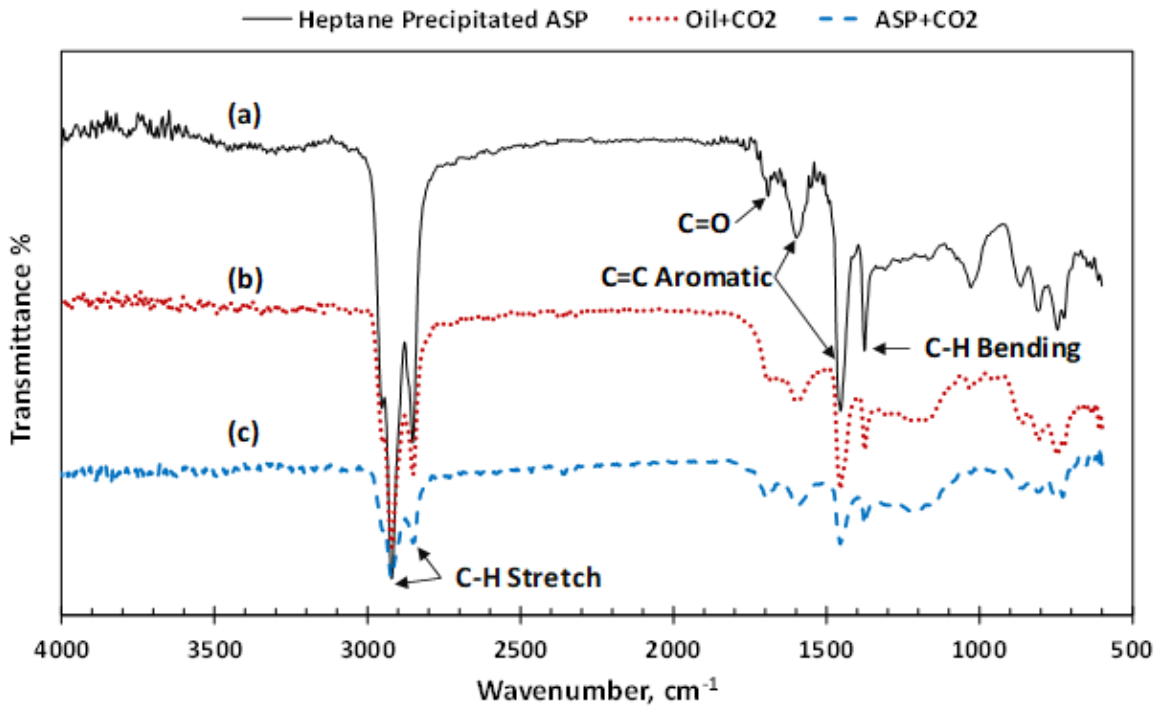

Figure 17. FTIR Spectra of (A) the Asphaltenes C without CO_2 Injection, (B) the Asphaltenes That Were Precipitated from Crude Oil C in Which CO_2 Was Injected to the Oil for 7 Days, and (C) the Asphaltenes C in Which CO_2 Was Injected to the Asphaltenes for 7 Days.

These results also indicate that the peak at 1690 cm^{-1} was observed in both pure and CO_2-reacted asphaltenes samples. Thus, CO_2 may not have any significant chemical reaction with these asphaltenes samples or not detectable by the FTIR spectrums. It is worth mentioning that the FTIR spectra of tested oil samples were not altered significantly after the addition of CO_2 which is indicative of the fact that asphaltene is the only portion of the crude oil that may participate in a chemical reaction with CO_2.

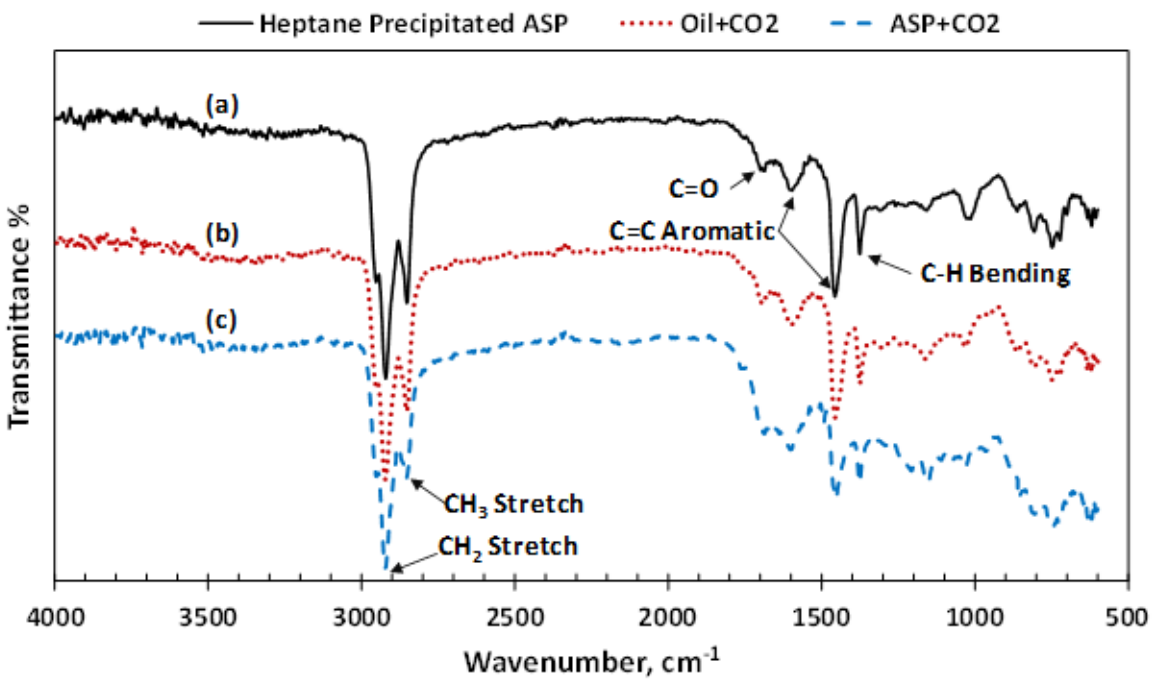

Figure 18. FTIR Spectra of (A) the Asphaltenes D without CO_2 Injection, (B) the Asphaltenes That Were Precipitated from Crude Oil D in Which CO_2 Was Injected to the Oil for 7 Days, and (C) the Asphaltenes D in Which CO_2 Was Injected to the Asphaltenes for 7 Days.

Characterizing the Functional Group Formed by CO_2 Injection

To identify the primary functional groups in asphaltenes **A** that reacted with CO_2 and resulted in the formation of a detected carbonyl functional group, several identification tests were carried out. Most of the common bases can react with CO_2 and generate new functional groups, however, the DABCO base that is selected for this experiment does not have any chemical reaction with CO_2. The function of this base (same as the other bases) is collapsing the H-bonded ion pair that existed in the asphaltenes structure (Cecchi et al. 2006). In other words, it can capture asphaltenes acidic hydrogens. This experiment is conducted to identify the existence of any hydroxyl groups, such as alcohols or phenols, in CO_2-reacted asphaltenes and to determine the functional group that detected the carbonyl group belongs to.

The base was added to the solution of asphaltenes and toluene, then CO_2 was injected into the solution and reacted for 3 days. **Figure 19** shows the FTIR spectrums of CO_2-reacted asphaltenes **A** in the absence and presence of DABCO. No significant differences between these two spectra were observed. Therefore, asphaltenes **A** that was reacted by CO_2 may not contain any acidic hydrogen groups such as, alcohol, and carboxylic acid functional groups. These observations are indicating that the generated carbonyl group belongs to either amide or aldehyde functional groups (McMurry et al. 2010). On the other hand, aldehyde can only be formed from the reaction of CO_2 with alcohol or phenol compounds. As a result, since we previously showed that the asphaltenes sample does not consist of any alcohol, the only functional group that can be assigned to the generated carbonyl bond is the amide functional group.

Due to the generation of aldehydes from alcohol groups, the CO_2-reacted asphaltenes **A** could not have aldehydes too. In this experiment, the concentration of the solution of CO_2-reacted asphaltenes **A** and DABCO base was 30% more than the solution without the base. Consequently, the peak of 1690 cm^{-1} related to the first solution is more intensified compared to the one without the base as seen in **Figure 19**.

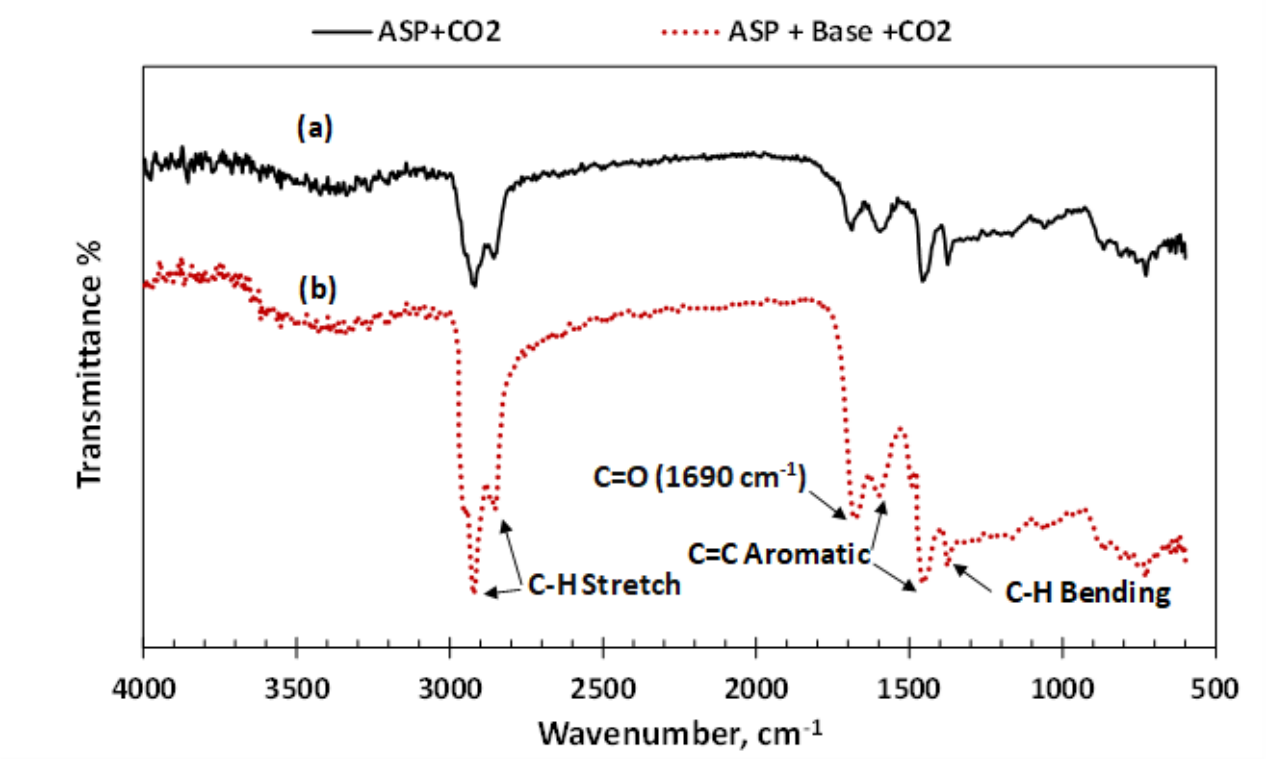

Figure 19. FTIR Spectra of the Asphaltenes A in Which CO_2 Was Injected to the Asphaltenes (A) without DABCO Base and (B) with DABCO Base.

To further investigate the system, another identification test was conducted using hydrochloric acid. CO_2-reacted asphaltene was mixed with HCl for 30 min at 140°F. Then the solution was dried and its FTIR spectrum was collected. **Figure 20** shows the FTIR spectrums of CO_2-reacted asphaltenes before and after the addition of HCl. Two significant dissimilarities can be observed in the FTIR spectrums: first, the carbonyl peak at 1690 cm^{-1} (which was generated after the reaction of asphaltenes with CO_2) disappeared and the new peak at 1706 cm^{-1} was formed that can be assigned to C=O stretching vibration of the carboxylic acid group; second, a new broad peak in the region of 3200-3500 cm^{-1} was generated which can be assigned to N-H stretching vibrations. Analysis of these changes can be done by looking at the hydrolysis and degradation reaction of the amide group in the presence of HCl has shown in **Figure 12**. This reaction shows

that the amide hydrolysis generates carboxylic acid and amine groups. The associated FTIR peaks of these functional groups (1706 and 3200-3500 cm^{-1} for C=O stretching of carboxylic acid and N-H band of amine, respectively) are in the same regions of the generated observed peaks in the FTIR spectrum of CO_2-reacted asphaltenes after reaction with HCl. These results are in good agreement with the first identification tests due to the fact that aldehydes would not hydrolyze in the presence of HCl. Hence, the coupling of base addition and qualitative test observations prove the presence of amide in this asphaltene after carbon dioxide flooding.

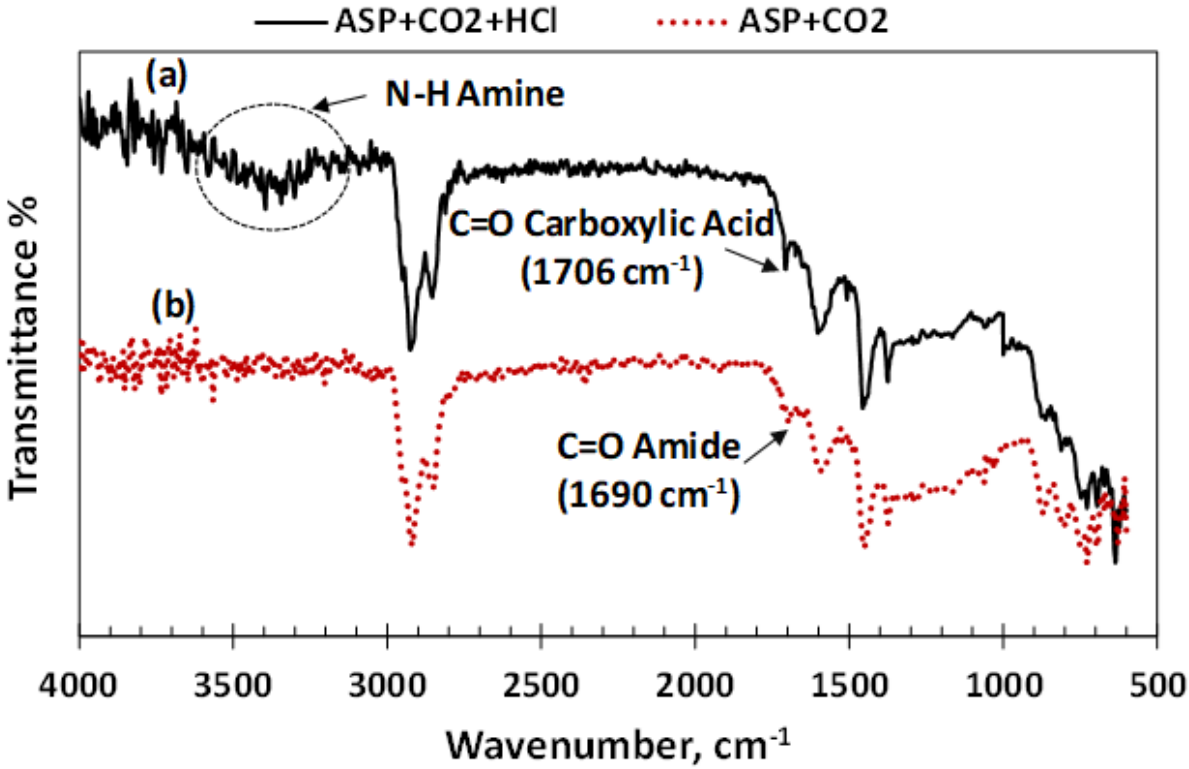

Figure 20. FTIR Spectra of the Asphaltenes A in Which CO_2 Was Injected to the Asphaltenes (A) After the Qualitative Test and (B) Before the Qualitative Test (HCl Addition).

It is worth noting that in FTIR, the conjugations of C=O groups of amides or carboxylic acids with aromatics or aliphatic groups shift the wavenumbers of carbonyl groups slightly to the right. Therefore, as the asphaltene is a complex and conjugated molecule, all wavelengths related

to carbonyl functional groups are shifted to the lower wavelengths compared to carbonyl groups of the simple and unconjugated molecules.

Control Test

As a control test, CO_2 was injected to toluene and its FTIR spectrum is compared with regular toluene to confirm that there is no reaction between solvent and CO_2. This is shown in **Figure 21**. No change was observed in the FTIR spectrum of toluene after the addition of CO_2. Therefore, carbon dioxide has no chemical reaction with toluene and the observed changes in the FTIR peaks originated from asphaltenes structural alteration.

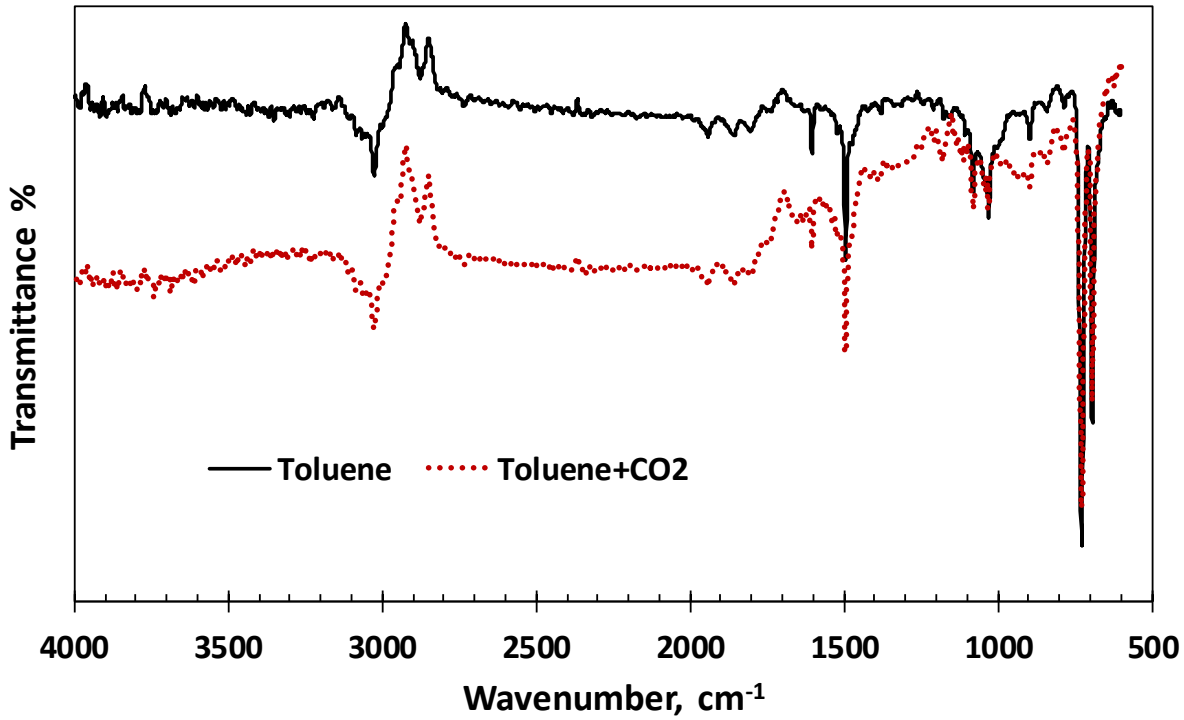

Figure 21. FTIR Spectra of Toluene in the Presence and Absence of CO_2.

N_2 was also injected into the solution of asphaltenes **A** and toluene for one week at 752°F to observe any possible changes in the asphaltenes chemical structures. **Figure 22** shows the FTIR spectrums of N_2-reacted asphaltenes and the original asphaltenes samples. The fact that no significant changes could be observed in these two spectrums implies that there is no chemical reaction between nitrogen and asphaltenes samples. However, asphaltene can have a chemical reaction with carbon dioxide.

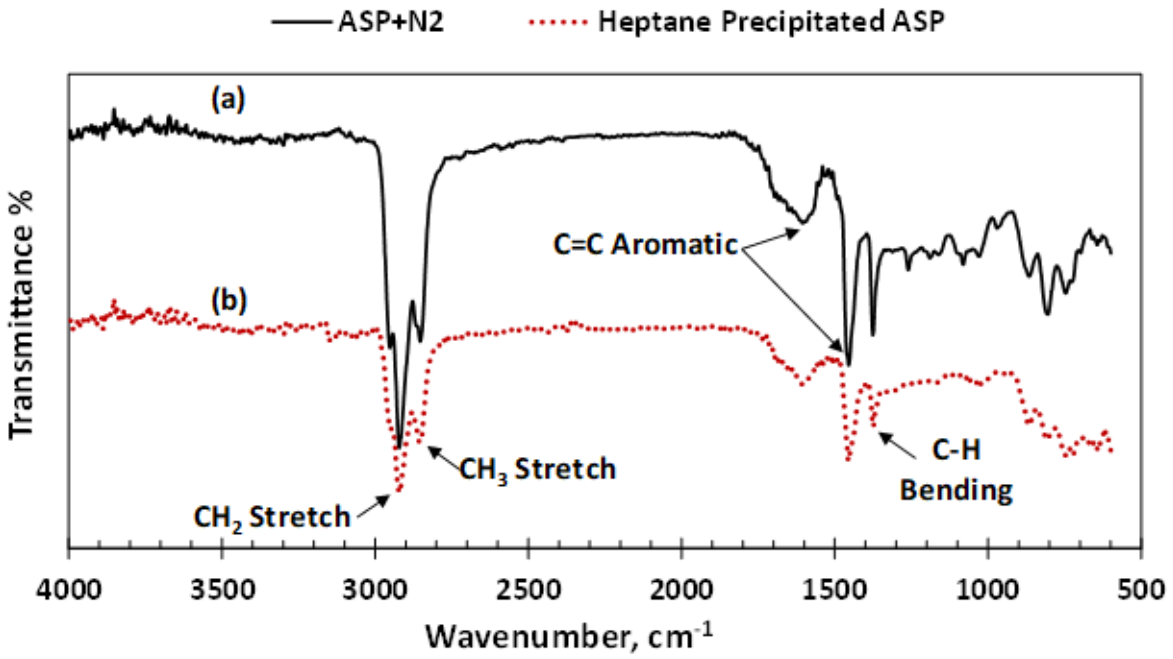

Figure 22. FTIR Spectra of the Asphaltenes A (A) in Which N_2 Was Injected to the Asphaltenes for 7 Days, and (B) without N_2 Injection.

Effects of CO_2 on Asphaltenes Stability

The stability of the asphaltenes samples in the model oil was determined directly by evaluating their precipitation onset points using a titration method. Based on the UV-Vis absorbance as a function of wavelength, the highest amount of absorbance signal was measured around 300 to 400 nm; thus, the absorbance of different samples at a wavelength of 350 nm was

plotted as a function of the n-heptane concentration. This method works in any other wavelengths in the range of 250-1100 nm; however, the highest differences between absorbance values are observed at 350 nm. The deviation from linearity parallels the onset point of the solution. To identify the appropriate onset point, the dilution effect should be adjusted. Before dilution effect elimination, the UV-Vis plot of absorbance as a function of the n-heptane volume percentage is linear. The samples were diluted two times. First, the model oil was diluted with different volumes of precipitant (n-heptane). Then, after centrifuge, the 1 ml of samples were diluted with 4 ml toluene. The dilution does not affect the asphaltenes onset point detection. Tavakkoli et al. (2015) suggest the method to remove the influence of dilution. The absorbance of fluid becomes excessively noisy. Hence it is critical to eliminate the dilution effect. To do so, during the sample's preparation, the mass of each liquid (precipitant and toluene) was measured. The exact volume of oil is also required. Due to the very low concentration of asphaltene in solution, the density of model oil is approximately equal to the density of toluene. By having the model oil and n-heptane volumes (cm^3), the dilution ratio of adding n-heptane to oil is calculated:

$$\text{Dilution ratio for n} - \text{heptane addition} = \frac{(\text{n}-\text{C7 volume}+\text{Model oil volume})}{\text{Model oil volume}} \quad (5)$$

Furthermore, for measuring the dilution ratio of 4 ml additional toluene, the toluene volumes are required. **Equation 6** is required for finding the dilution ratio of adding toluene to the 1 ml of supernatant liquid after centrifuge:

$$\text{Dilution ratio for toluene addition} = \frac{(\text{Toluene volume}+\text{Supernatant liquid volume})}{\text{Supernatant liquid volume}} \quad (6)$$

The overall dilution ratio for this method is calculated by multiplying the dilution ratio for n-heptane addition to the dilution ratio of toluene adding to the 1 ml of supernatant liquid after centrifuge. By multiplying the absorbance values at 350 nm to the overall dilution ratio, the corrected absorbance is calculated for each sample. Therefore, the dilution effect is removed from the UV-Vis graph.

Figure 23 shows the absorbance of 1 ml of model oil from asphaltenes **A** that were diluted with 4 ml toluene as a function of n-heptane volume%. The sharp decline of absorbance at 44 vol% of n-heptane indicates the onset point of asphaltenes precipitation. **Figure 24** shows the corresponding results for CO_2-reacted asphaltenes **A**. It can be seen from this plot that the onset point for the CO_2-reacted asphaltenes occurred after the addition of 26 vol% of n-heptane.

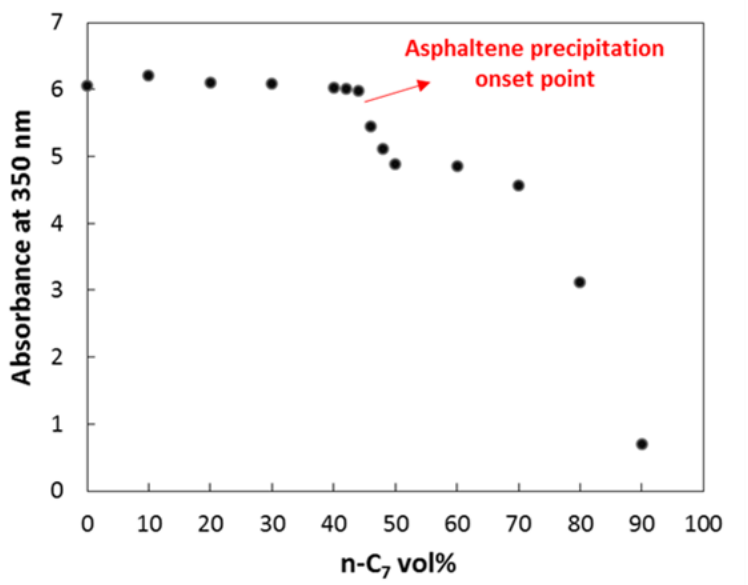

Figure 23. Results of the Absorbance at 350 Nm Vs N-Heptane Vol% from UV-Vis Spectroscopy Technique for Determination of Asphaltene Precipitation Onset Point from Model Oil (Asphaltenes A and Toluene) Diluted with N-C_7.

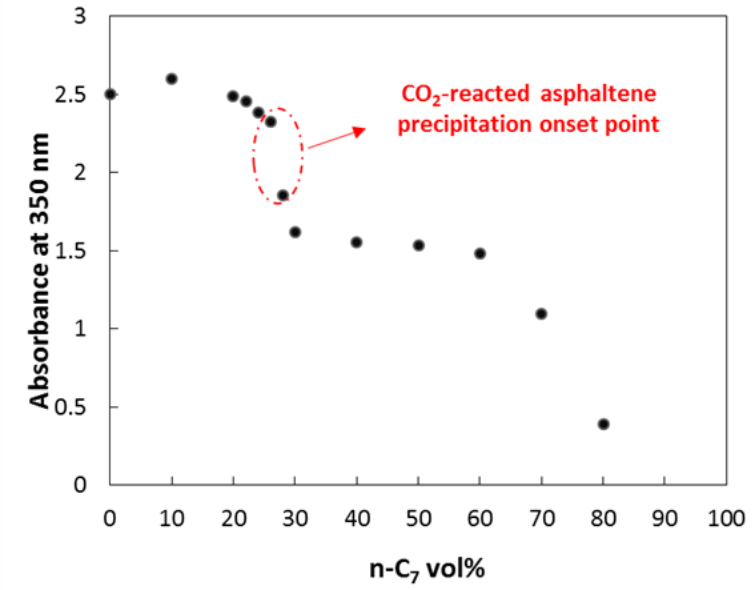

Figure 24. Results of the Absorbance at 350 Nm Vs N-Heptane Vol% from UV-Vis Spectroscopy Technique for Determination of Asphaltene Precipitation Onset Point from Model Oil (CO_2-Reacted Asphaltenes A and Toluene) Diluted with N-C_7.

The differences between the asphaltenes precipitation onset points, prove that carbon dioxide makes the asphaltene unstable. Therefore, the asphaltenes stability is correlated to its structure and functional groups. Formation of the amide functional group would result in an increasing asphaltene molecule's propensity toward forming clusters and aggregating. It consequently leads to a decrease in precipitation onset point.

The onset point of asphaltenes **C** and **D** were not changed after reaction with CO_2. As noted earlier, their chemical structures were not changed by CO_2 flooding. However, the onset point of asphaltene **B** (the one extracted from heavy crude oil) was changed slightly after reaction with CO_2. Since no significant change was observed in the FTIR spectrum of asphaltene **B** in the presence of CO_2, the alteration of its stability cannot be related to any significant chemical reaction.

As a result, such an observation can be explained by the possible interaction of CO_2 with the oil matrix.

CHAPTER IV

CONCLUSIONS

In this research study, several experiments were conducted to better understand the influences of carbon dioxide on the structure and stability of asphaltenes samples from four crude oils during the tertiary oil recovery. The differences between the structures and stabilities of n-C_7 and CO_2 asphaltenes were examined using FTIR and UV-Vis spectroscopy, respectively. Based on the obtained results, the following conclusions were drawn:

- Asphaltenes are the only portion of crude oil that may have a chemical reaction with carbon dioxide. However, the chemical reaction of CO_2 with diverse asphaltenes are completely different. There is not a meaningful correlation between the crude oil composition (SARA) and the asphaltenes structural changes by CO_2. This is attributed to the functional groups of asphaltenes.
- Based on FTIR spectroscopy and acid/base identification tests, the asphaltenes **A** contain amine groups and it does not have any hydroxyl groups. After CO_2 injection, its chemical structure was changed, and the amide functional group appeared in the FTIR spectrum.
- The new functional group that was created by CO_2 treatment induces the reduction in onset of asphaltenes precipitation. It was observed that the amide functional group disturbed and decreased asphaltenes stability as well.
- It was also shown that although asphaltenes **B** did not react with CO_2 chemically, however, its stability was impaired after exposure to CO_2.

It can be concluded from these results that depending on the nature of the asphaltenes, its solubilization or stabilization can be done to prevent asphaltenes associated problems. The main achievement of this work is using reliable techniques for identifying the new functional groups after CO_2 injection that has a direct influence on asphaltenes instability. Further, these results stipulate the importance of understanding the nature of asphaltenes destabilization mechanism by CO_2 to use any appropriate chemical methods or inhibitors to prevent asphaltenes related problems.

REFERENCES

Afra, S., Alrashidi, H. G., and Nasr-EL-Din, H. A. 2017. Interrelationship Between Asphaltene Precipitation Methods and Asphaltene Characteristics and Self-Association Behavior. Presented at the SPE Latin America and Caribbean Petroleum Engineering Conference, Buenos Aires, Argentina, 17-19 May. SPE-185542-MS. https://doi.org/10.2118/185542-MS.

Akmaz, S., Iscan, O., Gurkaynak, M. A. et al. 2011. The structural characterization of saturate, aromatic, resin, and asphaltene fractions of Batiraman crude oil. *J Petroleum Science and Technology* **29** (2): 160-171. https://doi.org/10.1080/10916460903330361.

Alboudwarej, H., Pole, D., Svrcek, W. Y. et al. 2005. Adsorption of Asphaltenes on Metals. *Industrial & engineering chemistry research* **44** (15): 5585-5592. https://doi.org/10.1021/ie048948f.

Behar, E., Hasnaoui, N., Achard, C. et al. 1998. Study of Asphaltene Solutions by Electrical Conductivity Measurements. *Review of the French Institute of Petroleum* **53** (1): 41-50. https://doi.org/10.2516/ogst:1998007.

Borton, D., Pinkston, D. S., Hurt, M. R. et al. 2010. Molecular Structures of Asphaltenes Based on the Dissociation Reactions of Their Ions in Mass Spectrometry. *Energy & Fuels* **24** (10): 5548-5559. https://doi.org/10.1021/ef1007819.

Brouwer, P. 2006. Theory of XRF: Getting acquainted with the principles. PANalytical BV.

Cao, M. and Gu, Y. 2013. Oil recovery mechanisms and asphaltene precipitation phenomenon in immiscible and miscible CO_2 flooding processes. *Fuel* **109**: 157-166. https://doi.org/10.1016/j.fuel.2013.01.018.

Cecchi, L., De Sarlo, F., and Machetti, F. 2006. 1,4-Diazabicyclo[2.2.2]octane (DABCO) as an Efficient Reagent for the Synthesis of Isoxazole Derivatives from Primary Nitro Compounds and Dipolarophiles: The Role of the Base. *European J Organic Chemistry* **2006** (21): 4852-4860. https://doi.org/10.1002/ejoc.200600475.

Coelho, R. R., Hovell, I., Moreno, E. L. et al. 2007. Characterization of functional groups of asphaltenes in vacuum residues using molecular modelling and FTIR techniques. *J Petroleum Science and Technology* **25** (1-2): 41-54. https://doi.org/10.1080/10916460601054198.

Cunico, R. L., Sheu, E. Y., and Mullins, O.C. 2004. Molecular weight measurement of UG8 asphaltene using APCI mass spectroscopy. *J Petroleum Science and Technology* **22** (7-8): 787-798. https://doi.org/10.1081/LFT-120038719.

Dong, Z. X., Wang, J., Liu, G. et al. 2014. Experimental study on asphaltene precipitation induced by CO_2 flooding. *J Petroleum Science* **11** (1): 174-180. https://link.springer.com/article/10.1007/s12182-014-0329-2.

Dutta Majumdar, R., Bake, K. D., Ratna, Y. et al. 2016. Single-core PAHs in petroleum-and coal-derived asphaltenes: size and distribution from solid-state NMR spectroscopy and optical absorption measurements. *Energy & Fuels* **30** (9): 6892-6906. https://doi.org/10.1021/acs.energyfuels.5b02815.

Escobedo, J. and Mansoori, G. A. 1995. Viscometric Determination of the Onset of Asphaltene Flocculation: A Novel Method. *SPE Prod & Fac* **10** (02): 115-118. SPE-28018-PA. https://doi.org/10.2118/28018-PA.

Fotland, P., Anfindsen, H., and Fadnes, F. H. 1993. Detection of Asphaltene Precipitation and Amounts Precipitated by Measurement of Electrical Conductivity. *Fluid Phase Equilibria* **82**: 157-164. https://doi.org/10.1016/0378-3812(93)87139-R.

Gabrienko, A. A., Martyanov, O. N., and Kazarian, S. G. 2016. Behavior of Asphaltenes in Crude Oil at High-Pressure CO_2 Conditions: In Situ Attenuated Total Reflection–Fourier Transform Infrared Spectroscopic Imaging Study. *Energy & Fuels* **30** (6): 4750-4757. https://doi.org/10.1021/acs.energyfuels.6b00718.

Gharfeh, S., Yen, A., Asomaning, S. et al. 2004. Asphaltene flocculation onset determinations for heavy crude oil and its implications. *J Petroleum Science and Technology* **22**(7-8): 1055-1072. https://doi.org/10.1081/LFT-120038711.

Godec, M. L., Kuuskraa, V. A., and Dipietro, P. 2013. Opportunities for using anthropogenic CO_2 for enhanced oil recovery and CO_2 storage. *Energy & Fuels* **27** (8): 4183-4189. https://doi.org/10.1021/ef302040u.

Goual, L. and Firoozabadi, A. 2002. Measuring Asphaltenes and Resins, and Dipole Moment in Petroleum Fluids. *AIChE J* **48** (11): 2646-2663. https://doi.org/10.1002/aic.690481124.

Hosseini, A., Zare, E., Ayatollahi, S. et al. 2016. Electrokinetic behavior of asphaltene particles. *Fuel* **178**: 234-242. https://doi.org/10.1016/j.fuel.2016.03.051.

Hu, Y. F., Li, S., Liu, N. et al. 2004. Measurement and corresponding states modeling of asphaltene precipitation in Jilin reservoir oils. *J Petroleum Science and Engineering* **41** (1-3): 169-182. https://doi.org/10.1016/S0920-4105(03)00151-7.

Ibrahim, H. H. and Idem, R. O. 2004. Correlations of Characteristics of Saskatchewan Crude Oils/Asphaltenes with Their Asphaltenes Precipitation Behavior and Inhibition Mechanisms: Differences between CO_2- and n-Heptane-Induced Asphaltene Precipitation. *Energy & Fuels* **18** (5): 1354-1369. https://doi.org/10.1021/ef034044f.

Kokal, S. L., Najman, J., Sayegh, S. G. et al. 1992. Measurement and Correlation of Asphaltene Precipitation from Heavy Oils by Gas Injection. *J Can Pet Technol* **31** (04). PETSOC-92-04-01. https://doi.org/10.2118/92-04-01.

Kokal, S. L. and Sayegh, S. G. 1995. Asphaltenes: The Cholesterol of Petroleum. Presented at Society of Petroleum Engineers, Bahrain, 11-14 March. SPE-29787-MS. https://doi.org/10.2118/29787-MS.

Koolen, H. H., Gomes, A. F., de Moura, L. G. et al. 2018. Integrative mass spectrometry strategy for fingerprinting and tentative structural characterization of asphaltenes. *Fuel* **220**: 717-724. https://doi.org/10.1016/j.fuel.2017.12.078.

Król, M., Minkiewicz, J., and Mozgawa, W. 2016. IR Spectroscopy Studies of Zeolites in Geopolymeric Materials Derived from Kaolinite. *J Molecular Structure* **1126**: 200-206. https://doi.org/10.1016/j.molstruc.2016.02.027.

Leontaritis, K. J. and Mansoori, G. A. 1988. Asphaltene Deposition: A Survey of Field Experiences and Research Approaches. *J Petroleum Science and Engineering* **1** (3): 229-239. https://doi.org/10.1016/0920-4105(88)90013-7.

Leyva, C., Ancheyta, J., Berrueco, C. et al. 2013. Chemical characterization of asphaltenes from various crude oils. *J Fuel Processing Technology* **106**: 734-738. https://doi.org/10.1016/j.fuproc.2012.10.009.

Li, Y., Sorribes, I., Yan, T. et al. 2013. Selective Methylation of Amines with Carbon Dioxide and H_2. *Angewandte Chemie International Edition* **52** (46): 12156-12160. https://doi.org/10.1002/anie.201306850.

Magruder, J. B., Stiles, L. H., and Yelverton, T. D. 1990. Review of the Means San Andres Unit CO_2 Tertiary Project. *J Petroleum Technology* **42** (05): 638-644. SPE-17349-PA. https://doi.org/10.2118/17349-PA.

Mansur, C. R., Guimaraes, A. R., Gonzalez, G. et al. 2009. Determination of the Onset of Asphaltene Precipitation by Visible Ultraviolet Spectrometry and Spectrofluorimetry. *Analytical Letters* **42** (16): 2648-2664. https://doi.org/10.1080/00032710903243612.

McKenna, A. M., Donald, L. J., Fitzsimmons, J. E. et al. 2013. Heavy petroleum composition. 3. Asphaltene aggregation. *Energy & Fuels* **27** (3): 1246-1256. https://doi.org/10.1021/ef3018578.

McMurry, J., Ballantine, D. S., Hoeger, C. A. et al. 2010. *Fundamentals of General, Organic, and Biological Chemistry*, Sixth Edition: Pearson Education.

Melendez, L. V., Lache, A., Orrego-Ruiz, J. A. et al. 2012. Prediction of the SARA Analysis of Colombian Crude Oils using ATR–FTIR Spectroscopy and Chemometric Methods. *J*

Petroleum Science and Engineering **90**: 56-60. https://doi.org/10.1016/j.petrol.2012.04.016.

Mohammed, S. and Gadikota, G. 2019. The influence of CO_2 on the structure of confined asphaltenes in calcite nanopores. *Fuel* **236**: 769-777. https://doi.org/10.1016/j.fuel.2018.08.124.

Moreira, L. F. B., Lucas, E. F., and González, G. 1999. Stabilization of Asphaltenes by Phenolic Compounds Extracted from Cashew-Nut Shell Liquid. *J Applied Polymer Science* **73** (1): 29-34. https://doi.org/10.1002/(SICI)1097-4628(19990705)73:1<29::AID-APP3>3.0.CO;2-O.

Mousavi-Dehghani, S. A., Riazi, M. R., Vafaie-Sefti, M. et al. 2004. An Analysis of Methods for Determination of Onsets of Asphaltene Phase Separations. *J Petroleum Science and Engineering* **42** (2-4): 145-156. https://doi.org/10.1016/j.petrol.2003.12.007.

Mullins, O. C. 2010. The modified Yen model. *Energy & Fuels* **24** (4): 2179-2207. https://doi.org/10.1021/ef900975e.

Mullins, O. C., Sabbah, H., Eyssautier, J. et al. 2012. Advances in asphaltene science and the Yen–Mullins model. *Energy & Fuels* **26** (7): 3986-4003. https://doi.org/10.1021/ef300185p.

O'Connor, C. 1970. Acidic and Basic Amide Hydrolysis. *Chemical Society* **24** (4): 553-564.

Okwen, R. T. 2006. Formation Damage by CO_2 Asphaltene Precipitation. *SPE International Symposium and Exhibition on Formation damage control*. SPE-98180-MS. https://doi.org/10.2118/98180-MS.

Pavia, D. L., Lampman, G. M., Kriz, G. S. et al. 2008. *Introduction to spectroscopy,* Third Edition: Cengage Learning.

Pinkston, D. S., Duan, P., Gallardo, V. A. et al. 2009. Analysis of Asphaltenes and Asphaltene Model Compounds by Laser-Induced Acoustic Desorption/Fourier Transform Ion Cyclotron Resonance Mass Spectrometry. *Energy & Fuels* **23** (11): 5564-5570. https://doi.org/10.1021/ef9006005.

Pomerantz, A. E., Hammond, M. R., Morrow, A. L. et al. 2009. Asphaltene molecular-mass distribution determined by two-step laser mass spectrometry. *Energy & Fuels* **23**(3): 1162-1168. https://doi.org/10.1021/ef8006239.

Qian, K., Edwards, K. E., Siskin, M. et al. 2007. Desorption and Ionization of Heavy Petroleum Molecules and Measurement of Molecular Weight Distributions. *Energy & Fuels* **21** (2): 1042-1047. https://doi.org/10.1021/ef060360t.

Rakhmatullin, I. Z., Efimov, S. V., Tyurin, V. A. et al. 2018. Application of high-resolution NMR (1H and 13C) and FTIR spectroscopy for characterization of light and heavy crude

oils. *J Petroleum Science and Engineering* **168**: 256-262. https://doi.org/10.1016/j.petrol.2018.05.011.

Ruiz-Morales, Y. 2002. HOMO− LUMO gap as an index of molecular size and structure for polycyclic aromatic hydrocarbons (PAHs) and asphaltenes: A theoretical study. I. *J Physical Chemistry A* **106** (46): 11283-11308. https://doi.org/10.1021/jp021152e.

Schuler, B., Meyer, G., Peña, D. et al. 2015. Unraveling the molecular structures of asphaltenes by atomic force microscopy. *J American Chemical Society* **137** (31): 9870-9876. https://doi.org/10.1021/jacs.5b04056.

Sheu, E. Y. 2002. Petroleum asphaltene properties, characterization, and issues. *Energy & Fuels* **16** (1): 74-82. https://doi.org/10.1021/ef010160b.

Shirokoff, J. and Lye, L. 2019. A Review of Asphalt Binders Characterized by X-ray Diffraction. *Innovations in Corrosion and Materials Science* **9** (1): 28-40. https://doi.org/10.2174/2352094909666190401205036.

Srivastava, R. K., Huang, S. S., and Dong, M. 1999. Asphaltene Deposition during CO_2 Flooding. *SPE Prod & Fac* **14** (04): 235-245. SPE-59092-PA. https://doi.org/10.2118/59092-PA.

Takahashi, S., Hayashi, Y., Takahashi, S. et al. 2003. Characteristics and impact of asphaltene precipitation during CO_2 injection in sandstone and carbonate cores: An investigative analysis through laboratory tests and compositional simulation. *SPE International Improved Oil Recovery Conference in Asia Pacific*. SPE-84895-MS. https://doi.org/10.2118/84895-MS.

Tavakkoli, M., Grimes, M. R., Liu, X. et al. 2015. Indirect Method: A Novel Technique for Experimental Determination of Asphaltene Precipitation. *Energy & Fuels* **29** (5): 2890-2900. https://doi.org/10.1021/ef502188u.

Verdier, S., Carrier, H., Andersen, S. I. et al. 2006. Study of pressure and temperature effects on asphaltene stability in presence of CO_2. *Energy & Fuels* **20** (4): 1584-1590. https://doi.org/10.1021/ef050430g.

Wang, J. and Buckley, J. S. 2003. Asphaltene stability in crude oil and aromatic solvents the influence of oil composition. *Energy & Fuels* **17** (6): 1445-1451. https://doi.org/10.1021/ef030030y.

Wang, S., Li, K., Chen, C. et al. 2019. Isolated mechanism study on in situ CO_2 EOR. *Fuel* **254**: 115575. https://doi.org/10.1016/j.fuel.2019.05.158.

Wattana, P., Wojciechowski, D. J., Bolaños, G. et al. 2003. Study of asphaltene precipitation using refractive index measurement. *J Petroleum Science and Technology **21*** (3-4): 591-613. https://doi.org/10.1081/LFT-120018541.

Zanganeh, P., Ayatollahi, S., Alamdari, A. et al. 2012. Asphaltene Deposition during CO_2 Injection and Pressure Depletion: A Visual Study. *Energy & Fuels* **26** (2): 1412-1419. https://doi.org/10.1021/ef2012744.